Journal of Environmental Management, Volume 295, October 2021, Article number 113362
DOI:10.1016/j.jenvman.2021.113362

Visible light-conducting polymer nanocomposites as efficient photocatalysts for the treatment of organic pollutants in wastewater

Nafees Ahmad [1,2], Jerry Anae[1], Mohammad Zain Khan[2], Suhail Sabir[2], Xiao Jin Yang[3,4], Vijay Kumar Thakur[5], Pablo Campo[1], Frederic Coulon[1*]

[1] School of Water, Energy and Environment, Cranfield University, Cranfield, MK 43 0AL, UK

[2]Environmental Research Laboratory, Department of Chemistry, Aligarh Muslim University, Aligarh, India, 202002

[3]State Key Laboratory of Chemical Resource Engineering, Beijing Advanced Innovation Center for Soft Matter Science and Engineering, Beijing University of Chemical Technology, Beijing 100029, China

[4]State Key Laboratory of Organic-Inorganic Composites, Beijing University of Chemical Technology, Beijing, 100029, PR China

[5]Biorefining and Advanced Materials Research Centre, Scotland's Rural College, Edinburgh, EH9 3JG, UK

Abstract

This review compiles recent advances and challenges on photocatalytic treatment of wastewater using nanoparticles, nanocomposites, and polymer nanocomposites as photocatalyst. The review provides an overview of the fundamental principles of photocatalytic treatment along the recent advances on photocatalytic treatment, especially on the modification strategies and operational conditions to enhance treatment efficiency and removal of recalcitrant organic contaminants. The different types of photocatalysts along the key factors influencing their performance are also critically discussed and recommendations for future research are provided.

Keywords: Photocatalyst, polymer nanocomposites, organic contaminants, wastewater treatment, band gap

Outline

1 Introduction 4

2 Photocatalysis 9

2.1 Principle and mechanistic approach of photocatalysis 10

2.2 Ideal photocatalyst and light source 12

2.3 Combination of photodegradation and biodegradation of the organic pollutants 13

3 Polymer nanocomposites as photocatalyst 14

3.1 Enhancing conducting polymers activity 16

3.2 Polymer-semiconductor nanocomposites 19

3.2.1 Heterojunction (p-n, p-p,n-n type) mechanism 19

3.2.2 Z-scheme photocatalysis by conducting polymers 21

3.3 Polymer-Graphene and Multiwall Carbon Nanotube (MWCNT) composites 23

3.4 Conducting polymer-biopolymer composites 24

3.5 Polymer- Clay nanocomposites (PCNs) 26

4 Factors affecting the photocatalytic degradation of organic pollutants in wastewater 28

4.1 Effect of photocatalyst amount 29

4.2 Size and morphology of the photocatalyst 29

4.3 Surface area 30

4.4 Reaction temperature 30

4.5 Concentration and nature of organic pollutants 31

4.6 Effect of pH 32

4.7 Inorganic ions present in the water 32

4.8 Effect of dopant 33

4.9 Effect of light intensity, wavelength and the irradiation time 34

5 Conclusions and Future Perspectives 35

Acknowledgements

References

1 Introduction

Water is an essential resource for the survival of human being and animal on earth. Even though, 70% of the world is covered by water, only 2.5% of water is considered as fresh that can be used for drinking water (Rajasulochana et al. 2016). Scarcity of drinking water has become a challenging issue worldwide due to contamination of water bodies by toxic pollutants discharged from industries. Around the globe, billions of populations lack fresh water for their basic needs. Rapid globalisation and industrialisation lead to higher production of a variety of novel and complex chemicals and the waste generated is directly discharged to the water streams (Kumari et al. 2019). The prime sources of water pollution include industrial wastes, mining activities, sewage, pesticides and chemical fertilizers, radioactive waste, and agricultural wastes (Khalaf et al. 2015 Habibi et al. 2020). About 2 million tons of industrial wastes are directly discharged to the water bodies without treatment, posing a serious threat to the environment (Bolisetty et al. 2019). The major contaminants associated with wastewater are summarised in Table 1 along with their permissible limits. Pollutant concentrations exceeding the permissible limits are considered as hazardous to human health and aquatic species. Due to the complex chemical structure and toxic functional groups of the pollutants, it is quite challenging to degrade or remove them via conventional techniques. Intensive research which includes physical, chemical, and biological methods has been developed and implemented to degrade and remove these pollutants (Table 2). While several studies reported optimal results, a major setback is that most of these methods can only be operated up to certain contaminants concentration limits and under pH, solubility, and favourable conditions. Further to this, common barriers include high cost and high energy demand (Natrajan et al. 2018).

Table 1: Pollutants present in wastewater with a permissible concentration in wastewater (Ye et al. 2019)

S. No.	Pollutants	Toxic concentration for Human health and aquatic species	Challenges in removal
1	Organic dyes (cationic and anionic dyes)	>1ppm	Stability and non-biodegradable nature
2	Aromatic compounds (phenol derivatives, toluene, xylene)	Benzene >0.01ppm Toluene >0.7ppm Xylene> 0.5ppm	Stable and very difficult to oxidize
3	PAHs (Polynuclear aromatic hydrocarbons)	>0.0007ppm	Non-biodegradable in nature, Low recovery while using membrane filtration, selection of specific adsorbents
4	Fertilizers and pesticides	>0.3ppm	Nitrogen and phosphorus-based fertilizes released form industries contain a very higher COD value. Variability of physical pesticides structure and pH of pesticides contaminated water (range 0.5 -14)
5	Heavy metals	As >0.01ppm Cd > 0.003ppm Cr > 0.05ppm Cu >2ppm Pb>0.01ppm Hg>0.006ppm Ni >0.07ppm Zn >3ppm	non-biodegradable nature
6	PPCPs	It is found in ng/l-µg/l in wastewater and exact concentration for each PPCPs are not specified as reported	Persistence and hydrophilic nature
7	Aqueous solution of NH_3 or NH_4^+	>0.2ppm	Specific environment (pH, alkalinity, and temperature) for nitrification and de-nitrification

There are however few emerging methods such as advanced oxidation process (photocatalysis), bio-sorption, biomass, membrane-filtration processes by nanofiltration used for the removal of organic pollutants(Gaur et al. 2018, Kumari et al. 2020, Anjum et al. 2019, Koutavarapu et al. 2021, Babu et al. 2021,Reddy et al. 2021). Among these processes, the photocatalytic process is considered as the most promising for the degradation/removal of organic pollutants. Apart from wastewater treatment, photocatalysis can also be used for energy generation, hydrogen production and carbon dioxide reduction (Asadzadeh et al. 2020, Akhundi, et al. 2019, Akhundi et al. 2020,

Nasir et al. 2019). However, research is still needed for optimising the process efficiency and especially on identifying and selecting photocatalysts for high efficiency and activity.

Table2: Advantages and disadvantages for the degradation of dyes, pesticides, pharmaceutical and personal care products (PPCPs) and polycyclic aromatic hydrocarbons (PAHs)

Methods	Types	Advantages	Disadvantages	References
–Chemical	• Advanced Oxidation Process • Oxidation • Electrochemical Destruction Hydrolysis • Photo-Fenton, • Ozonation • Chlorination • Ultraviolet Irradiation	• Fast process, • Highly efficient, • Degrade the pollutants completely	• High cost, • Complex Process, • Formation of toxic by-products	Katheresan et al. 2017, Forgacs et al., 2004 ; Gupta et al. 2009 Hameed et al. 2007
Physical	• Adsorption • Membrane filtration • Coagulation and flocculation • Air stripping • Ion exchange • Reverse osmosis • Nanofiltration and Ultrafiltration	• Quick process • and efficient	• Cannot degrade the pollutants completely, • Generation of by-products	Hethnawi et al. 2017, Holkar et al. 2016
Biological	• Aerobic and anaerobic microbial degradation • Membrane bioreactor • Algae degradation • Enzyme degradation • Pure and mixed culture (Mixture of algae bacteria and fungi)	• Cheap, efficiently degraded the various types of dyes and other contaminants, • Reusable	• High cost, Slow process • Formation of toxic by-products, • Unstable system	Adegoke et al. 2015, Joshni et al. 2011

For this purpose, a wide range of visible light active photocatalysts have been developed including semiconductor nanoparticles, reduced graphene oxide, multi and singled walled carbon nanotubes (MWCNTs, SWCNTs), metal organic frameworks (MOFs), covalent organic frameworks (COFs), various types of clays, biodegradable polymers (i.e. chitosan, chitin, cellulose and gelatine) to form heterojunction with conducting polymers (Table 3).

Table 3: Example of various photocatalyst reported in previous literature

	Photocatalyst	Band gap	Light Intensity	Targeted pollutants	Effic.	Exposure Time (Min)	Reference
1	g-C_3N_4/TiO_2	2.9eV	LED (20 W)	Reactive Red 4	100%	60	Azami et al. 2020
2	3D hierarchical flower-like TiO2	3.2 eV	UV Lamp (20 W)	Phenol	97%	120	Tian et al. 2011
3	ZnO	3.2 eV	UV Lamp (11W)	Methylene Blue	80%	120	Moghaddas et al. 2020
4	WO3/g-C3N4	WO3-2.68 eV g-C_3N_4-2.7 eV	Xenon Lamp (300 W)	Methylene Blue	97%	120	Huang et al. 2013
5	Fe_2O_3/SiO_2	2.2 eV	Metal Halide Lamp (400 W)	Methylene Blue, Congo Red	88%	180	Mandal et al. 2019
6	SnO_2-ZnO QD-g-C_3N_4	g-C_3N_4 - 2.7 eV, ZnO- 3.2eV, SnO_2- 3.5 eV	Xenon Lamp (300 W)	Rhodamine B	99%	60	Vattikutti et al.2018
7	$ZnFe_2O_4$-ZnO	3.21-2.0 eV	Halogen Lamp (500 W)	Methylene Blue, Methyl Orange	98% 99%	300 360	Rameshbabu et al. 2016
8	WO_3-ZnO	2.83eV	UV Lamp (6 W)	Direct Blue-15	86.9	120	Ebrahimi et al. 2019
9	CuO-ZnO	3.16-3.09eV	Solar Light (850 W/cm^2)	Rhodamine 6G, Methylene Blue, Methyl Orange	78.9% 93.2% 90.1%	80 40 60	Singh et al. 2020
10	BiOBr-Ag-Ppy	2.72eV	Halogen Lamp (150 W)	Malachite Green, Phenol	97%	60	Liu et al. 2018
11	MnO_2, Polythiophene-MnO_2	2.0- 1.52eV	Sun Light Irradiation	Malachite Green, Trichlorophenol	91% 93%	80	Zia et al. 2020
12	TiO_2(B)-CdS	2.24eV	Tungsten Lamp (300 W)	Rhodamine B	91.9%	30	Cheng et al. 2020
13	Ag_3PO_4/$BiVO_4$	Ag_3PO_4-2.26eV $BiVO_4$-2.98eV	Xenon Lamp (300 W)	Tetracycline hydrochloride-phenol	91%	180	Gao et al. 2020
14	Cu_2O-$BiVO_4$-WO_3	Cu_2O- 2.0-2.5eV, $BiVO_4$-2.4 eV WO_3-2.5-3.0 eV	Tungsten Lamp, 100W	Sulfasalazine	89.5%	50	Omrani et al. 2020
15	Sb_2S_3/α-Ag_2WO_4	2.96-2.61 eV	Halogen Lamp (300W)	Methylene Blue	91.2%	60	Ayappan et al. 2020
16	TiO_2-ZrO_2	TiO_2-3.26 eV ZrO_2- 3.435eV	Mercury Lamp (125W)	Methyl Orange	98%	60	Zhang et al. 2016
17	SnO_2/BiOBr	SnO_2-3.48 eV BiOBr-2.58 eV	LED (5 W)	Rhodamine B, Crystal violet	98.2% 95%	40 70	Liu et al. 2018
18	$ZnFe_2O_4$–C_3N_4	$ZnFe_2O_4$-1.9eV C_3N_4-2.7eV	Xenon Lamp (500 W)	Orange II	97%	240	Yao et al. 2014
19	Bacterial cellulose/ZnO	2.8-2.89eV	UV light	Methyl Orange	91%	120	Wahid et al. 2019
20	BiOBr/TiO_2	2.1eV	Solar Radiation	Ciprofloxacin	100%	150	Rashid et al. 2019
21	Graphene Oxide/Ag_3O_4	Ag3O4- 2.3eV	500 W Xe lamp	Naphthalene, Phenanthrene	98.2% 82.1%	5 7	Yang etal. 2018

				Pyrene	100%	0.5	
22	Fe_3O_4-TiO2/rGO	Fe_3O_4- 1.4 eV TiO_2-3.2eV	Sunlight, Visible light and UV light	Atrazine	99%	40	Boruah et al. 2020
23	SnO_2-ZnS	SnO_2-3.8eV ZnS-3.1eV	High-pressure mercury lamp	Acetaminophen Carbamazepine Metoprolol Triclosan	70% 40% 67% 40%	120	Hojamberdiev et al. 2020
24	Ag_2S-NiO-ZnO	NiO-ZnO-3.0eV Ag2S-NiO-ZnO-2.4eV	500 W Halogen lamp	Rhodamine B	45% 95%	120	Shafi et al. 2019
25	g-C_3N_4-$Bi_2O_2CO_3$	g-C_3N_4-2.7eV $Bi_2O_2CO_3$-3.5eV	1000W Xe lamp	Tetracyclin Tetracyclin hydrochloride Oxytetracyclin Congo red Methyl orange Malachite green Methylene Blue	85.5% 96.2% 99.2% 88.9%	360	Zhao et al. 2019
26	$NaBiS_2$-ZnO	$NaBiS_2$ -1.25eV ZnO- 3.4eV	Solar light	tetracycline	98%	90	Koutavarapu et al. 2021
27	Bi_2WO_6-ZnO	Bi_2WO_6-2.7eV ZnO-3.4eV	Solar light	Rh B	99%	50	Koutavarapu et al. 2021
28	MnO_2-Chitosan-Aluminium oxy hydroxide (MnO_2-C-Al(O)OH	MnO_2-1.7eV MnO_2-C-1.6eV MnO_2-C-Al(O)OH-1.3eV	500W Tungsten lamp	Acid Navy blue dye	88.8%	80	Sultana et al. 2020

The above-mentioned nanoparticles and nanocomposites have shown excellent photocatalytic activity toward the degradation of toxic organic pollutants. However, the toxicity of the photocatalyst must be studied before applying them in photocatalytic treatments.

Few nanoparticles such as ZnO, CuS, CdS, HgI_2, PbS (permissible limits are shown in Table 1) are known to be toxic in nature. The toxic concentration of these nanoparticles should be in permissible limits otherwise the photocatalysts itself will pollute the water as described by Ahmad et al (2019).

For the past 15 years, visible-light-driven nanoparticles combined with conducting polymers such as polypyrrole, polyaniline and polythiophene found much interest in wastewater treatment owing to their remarkable properties like high absorption coefficients, excellent electrical and optical activity and mechanical properties (Liang et al. 2019, Ahmad et al. 2017, Bano et al. 2019). These conducting polymers can be doped with various nanoparticles in the form of heterojunction to enhance conductivity and photocatalytic activity. In the heterojunction or composite form, these conjugated polymers act as electron donor and nanoparticles act as the electron acceptor. Despite these recent progresses, a critical review on conducting polymer and biopolymer composites as photocatalyst for the treatment of wastewater is still lacking. Therefore, this review summarises the different types of conducting polymers and composites used as photocatalyst for wastewater treatment along their advantages and limitations. This review also highlights the key advantages of the photocatalytic methods over other conventional methods.

2 Photocatalysis

Photocatalysis is a type of catalytic reaction carried out under the influence of light (ultraviolet or visible) that includes catalysis of photochemical reactions to activate the catalytic process. Photocatalysis covers two phenomena including photocatalytic decomposition (PCD) in the absence of O_2 and photocatalytic oxidation (PCO) with atmospheric O_2 as a direct participant to the reaction (Pirzada et al. 2018). Nowadays, photocatalysts that are active in visible light are frequently applied for photodegradation of pollutants as the sunlight spectrum constitutes a large portion of visible light

around 40% (Weon et al. 2019, Pardeshi et al. 2008). This heterogeneous photocatalysis appeared as a new emerging advanced oxidation process based on the two-step process of the photocatalysis. It adsorbs reactants and absorbs efficient photons ($h\nu \geq Eg$), simultaneously.

2.1 Principle and mechanistic approach of photocatalysis

A general photocatalytic mechanism for the degradation of pollutants is presented in Fig.1. The process starts with irradiation of the light with energy greater than the band gap energy of the photocatalyst. The first step is to approach the adsorption and desorption equilibrium between photocatalyst and pollutants in absence of the light and once the equilibrium is attained then photocatalyst is permitted to irradiate. Under the influence of light various process are supposed to happen: generation of an electron in the conduction band (CB) and holes in the valence band (VB), trapping of the electron, electron-hole recombination, electron transfer, reduction reaction with an electron acceptor at conduction band, hole transfer and oxidation reaction with a hole acceptor at the valence band. Under the influence of light, photocatalyst is excited and ejects electrons from the valence band to conduction band leaving behind holes in the valence band. These photogenerated charges carriers (e- and h+) may take a different path in the mechanism.

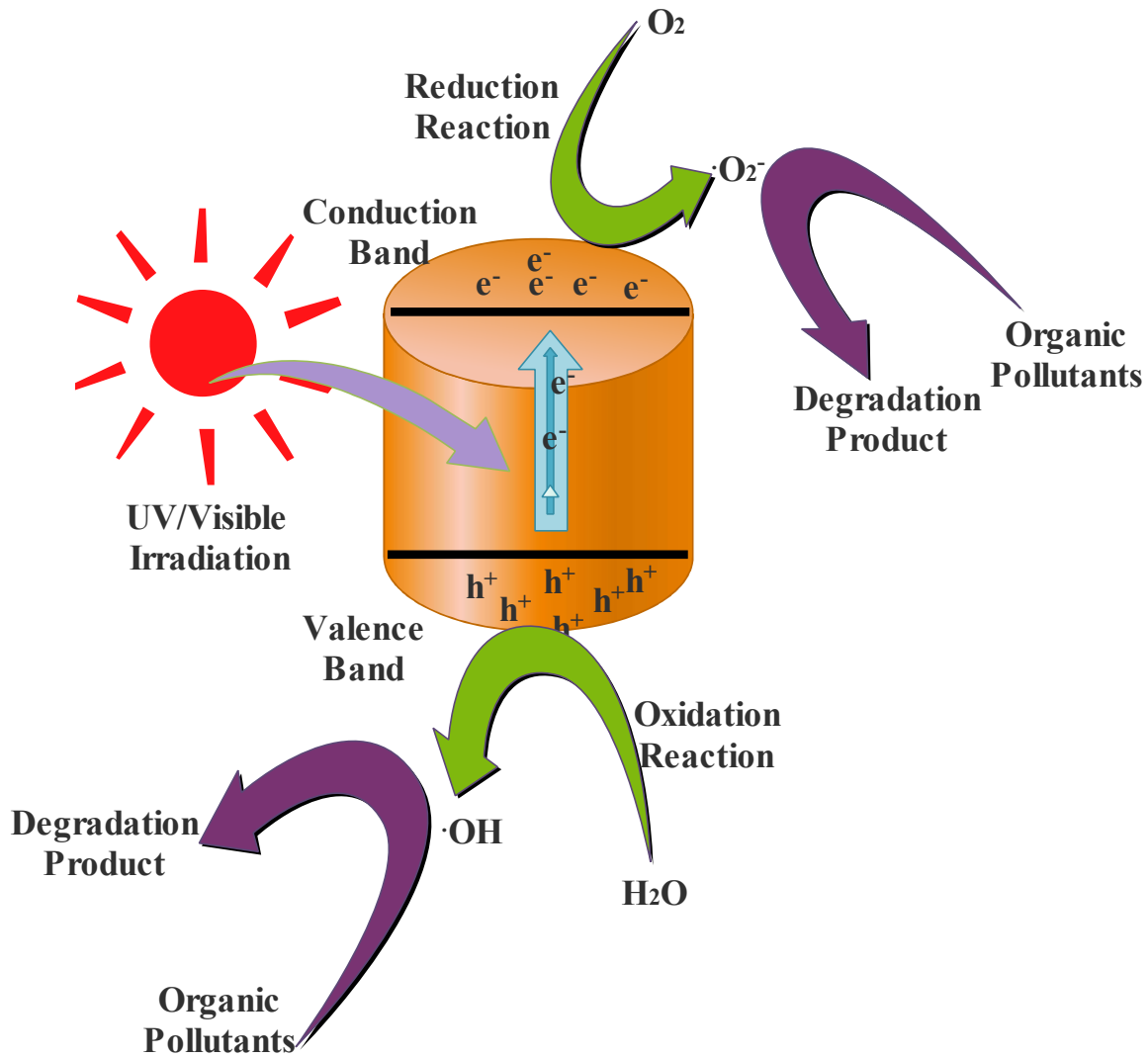

Fig.1: A general mechanism of photocatalysis for the degradation of organic pollutants

These charge carriers either can get caught in shallow traps or deep traps or can recombine radiatively or non-radiatively and release energy in the form of heat (Zhang et al. 1996). Photoredox reaction occurs at the catalyst surface by trapped electrons and trapped holes rather than from free ones in photocatalysis (Hoffmann et al 1995). Quantum efficiency for interfacial charge transfer can be ascertained between charge-carrier recombination and charge-carrier trapping (Zhang et al. 1996). Higher the charge-carrier recombination lower will be efficiency and vice versa. Further, electrons in CB are supposed to react to atmospheric oxygen supplied in reactor and form superoxide free radicals while holes in VB are oxidized by the H_2O molecules and form hydroxide free (·OH) radicals. Depending on the edge band potential of photocatalyst there is the possibility of formation of various

other reactive species such as superoxide and the peroxide radicals. These reactive species i.e. electron, holes, hydroxide radicals, and peroxide radicals, superoxide radicals are results for the degradation of organic pollutants. To achieve the higher efficiency of the catalyst, photocatalytic processes are assisted with the incorporation of hydrogen peroxide and ultrasonication (Huang et al. 2013, Aleboyeh et al. 2012) which are useful for the degradation of organic pollutants. A general mechanism is shown below in Equations (1-6) where 'S' represents the surface-active centre.

(i) Adsorption: Photocatalyst + Pollutants → Adsorption (Photocatalyst + pollutants) (1)

(ii) Photoexcitation (generation of e- and h+): Photocatalyst + hν → h^+ + e- (2)

(iii) Oxidation reaction by photogenerated holes (h+): S + h^+ → S^+ (3)

(iv) Reduction reaction by photogenerated electron (e^-): S^+ + e-→ S (4)

(v) Interaction of reactive oxygen species to pollutants: S^+ + Pollutants → $(S\text{-Pollutants})^+$ (5)

(vi) Degradation Product: $(S\text{-Pollutants})^+$ + e- → S + Degradation Products (6)

2.2 Ideal photocatalyst and light source

An ideal photocatalyst should be non-toxic, highly efficient, stable and must be inexpensive. Moreover, an ideal photocatalyst must have redox potential ($H_2O/\cdot OH$= -2.8eV) to generate hydroxyl radicals, a prime reactive oxygen species in the degradation of pollutants. Photocatalyst with higher surface area leads to faster photocatalytic reaction rates and show better activity, however, excess of nanoparticles may create surface defect and act as a recombination centre for photogenerated electron and lowers the catalyst activity (Li et al. 2013). Crystalline nature of the photocatalyst also results in higher photocatalytic activity as the defective sites will be less. Several photocatalysts have band gap energies in their electronic structure allowing catalysing a wide spectrum of chemical reactions. Photocatalyst with a wide range of band gaps is allowed to irradiate based on their band gap energy i.e. if the band gap energy of the photocatalyst is less than 3 eV then photocatalysts are supposed to absorb visible light irradiation and generates electron and holes however if the band gap energy is greater than 3 eV then the photocatalyst are supposed to irradiate with UV light to generate electron-

hole pairs. Conducting polymers being visible light active photocatalysts which have the band gap energy less than (Eg <3) has become an interesting topic for the photocatalytic purposes for wastewater treatment, carbon dioxide reduction and hydrogen generation.

2.3 Combination of photodegradation and biodegradation of the organic pollutants

Photocatalytic degradation and biodegradation have its own advantages and disadvantages for the when applied separately for the removal of wastewater pollutant. However, combination of these two methods has been found quite efficient in removal of pollutants and significant degradation was achieved as reported by some earlier literature (He et al. 2014, Wang et al. 2016 Song et al. 2020). In the combined process, the pollutants are first treated by photodegradation which is fast process and then the persistence intermediates are treated by biodegradation. For example, breakdown of azo bonds (–N=N–) of dyes into aromatic amines occurs after photodegradation and these intermediates are quite difficult to degrade by photodegradation method (Weldegebrieal, 2020, Kakarndee et al. 2018). These aromatic amines can be degraded to simpler compound via oxidative degradation using aerobic biodegradation process by the action of several oxygenase in aerobic conditions (Khan et al., 2020). Therefore, a combination of photodegradation and aerobic biodegradation could be an efficient combination for the treatment of pollutants (Song et al.2020, He et al. 2014). A combined mechanism of the photocatalytic degradation and biological degradation are shown in Fig. 2. In this mechanism the biological process is based on aerobic degradation. Several studies for the degradation of various pollutants are carried out by various research groups using integrated chemical-biological method for the degradation of diclofenac(He et al. 2014), tetracycline (Gomez-Pacheco et al. 2011), carbamazepine (Keen et al. 2012) and cefalexin (Estrada et al. 2012).

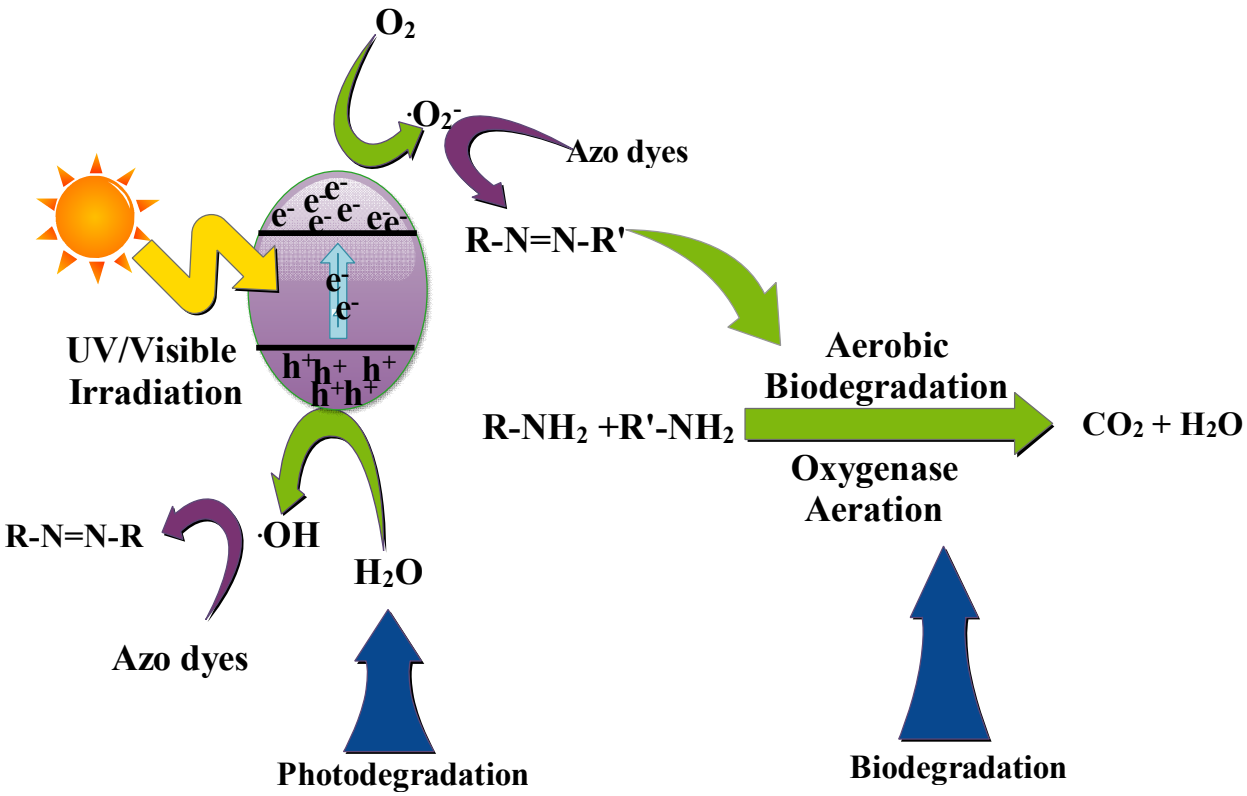

Fig.2: Combined mechanism of photodegradation and biodegradation of organic pollutants

3 Polymer nanocomposites as photocatalyst

For the last 15 years, conducting polymer nanocomposites due to their doping chemistry and narrower band gap are used as photocatalyst. Several conducting polymers have been used for the treatment of wastewater such as polyethylene, poly(vinyl pyrrolidone), polypyrrole, polyaniline, polythiophene, polyfurane, Nafion, Poly(3-hexylthiophene) (P3HT), Polyhydroxybutyrate (PHB), Poly(tetrafluoroethylene) (Geng et al. 2019, Ibanez et al. 2018, Kumar et al. 2020, Guo et al. 2019, Zhu et al. 2010). Among these polymers, polyaniline, polypyrrole, polythiophene and their composites have been frequently used as an efficient photocatalyst due to their easy synthesis and tuneable band gap energy (Steplin et al 2018, Zhao et al. 2017, Moosvi et al. 2017). These conducting polymers have been efficiently used as photocatalyst due to its visible-light-induced photocatalytic capability and tuneable band gap energy, redox properties, innocuous nature, inexpensive, chemically inert, higher surface area, and doping chemistry with the semiconductor nanoparticles. Moreover, due

to the hydrophobic nature of these polymers, organic pollutants are easily adsorbed on its surface and can easily be degraded (Mukhopadhyay et al. 2020).

For the treatment of wastewater, these conducting polymer doped with various nanoparticles can be used as membranes such as nanocomposites and thin-film nanocomposites, adsorbents such as conducting polymer and biopolymer supported activated carbon, ceramic material, magnetic oxides and clays and coagulants such as polymer clay composites, aluminium-silicate polymer composites and polymer hydrogels (Jhaveri et al. 2016, Worch 2012, Gao et al. 2002).Each of these materials (thin film, adsorbents, clays, and coagulants) is associated with certain limitations such as high cost of the membrane, limited for pollutants concentrations and selection of adsorbents according to concentration. These polymers nanocomposites with the properties of both polymers and nanomaterials generate electron-hole pairs when exposed to light of certain wavelength according to their band gap energy and subsequently form various reactive oxygen species. These conducting polymers easily absorb photons upon illumination of the visible light source and generate electron-holes pairs and then transfer these electrons from highest occupied molecular orbital (HOMO) to lowest unoccupied molecular orbital (LUMO) through π–$\pi*$ transition. In this process nanoparticles helps in suppressing the recombination rate of photogenerated electron and holes by accepting the electrons form polymers conduction band to its conduction band through interfacial charge transfer. In this way photogenerated electron in the conduction band will not able to recombine to photogenerated holes. Other factors that make polymer nanocomposites ideal for their applications in photocatalytic degradation are their stability and reusability (Silvestri et al. 2019; Neghi et al. 2019; Asgari et al. 2019; Di Mauro et al. 2017; Abinaya et al. 2019; Ahmad et al. 2019). They can be used several times (up to fifteen cycles) as they maintain their reactivity and available adsorption sites for the adsorption of pollutants.

3.1 Enhancing conducting polymers activity

Photocatalysts, when subjected to light, absorb a photon and subsequently generate the photo induced charge carriers (e- and h+). The excited electrons in the conduction band are in a most unstable state and will tend to occupy the stable state thus return to the valence band and recombine with photogenerated holes as shown in Fig. 3. So, to suppress recombination of the charge carries and achieve maximum efficiency, conducting polymers are either doped with nanoparticle, biopolymers, MOFs, COFs, reduced graphene oxide and clay to form a heterojunction or few oxidant are added during photocatalytic process. Oxidants such as $KBrO_3$, $(NH_4)_2S_2O_8$ and $K_2S_2O_8$ can also be added to suppress the recombination behaviour and promote the charge separation (Augugliaro et al. 2002, Abramovic et al. 2015). Authors have reported enhanced photocatalytic activity by adding oxidants (Bizani et al. 2006, Sobana et al. 2008). These oxidants trap the photogenerated electrons generated upon irradiation and inhibit the recombination of electrons to holes thus suppress the recombination process. Hydrogen peroxide (H_2O_2) is another oxidant commonly used as it plays a dual role in the photocatalytic process by generating by hydroxyl radicals, which are the prime reactive species in the photocatalytic mechanism and it can also be used to trap the electrons that inhibit the recombination of electron-hole pairs (Ajmal et al. 2014).However, H_2O_2 can be used up to a certain concentration otherwise it will retard the photocatalytic activity and generates peroxide radical that can trap photogenerated holes and therefore inhibit the photocatalytic activity (Sobana et al. 2008).

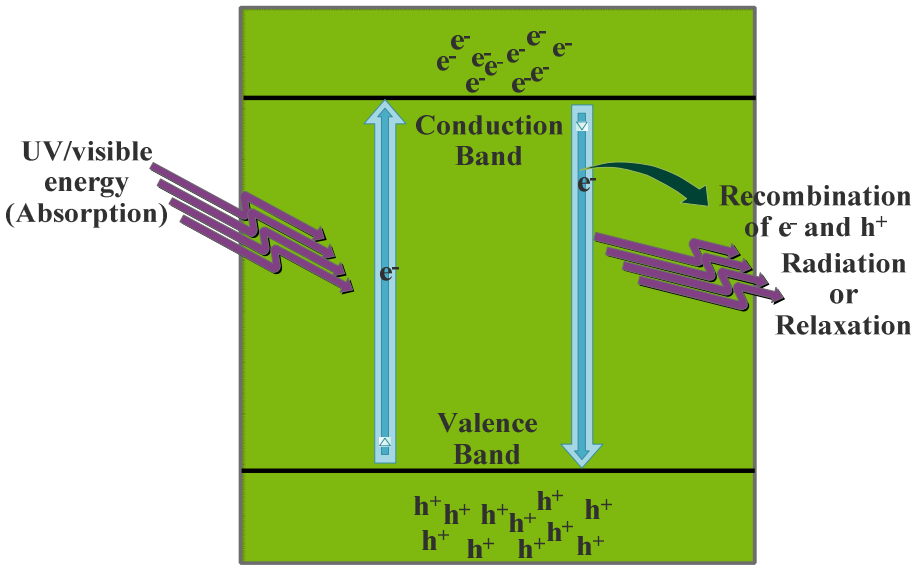

Fig.3: Recombination behaviour of photogenerated electrons and holes

Recombination of charge carriers can be studied by fluorescence spectroscopy (i.e. photoluminescence (PL) intensity). Photocatalyst which has lower electron-hole pair recombination would have lower PL intensity and show higher activity. Liu et al. (2018) reported the photocatalytic activity of the polypyrrole-BiOBr and compare the activity of photocatalyst with PL intensity with a various doping concentration of polypyrrole-BiOBr catalyst. Ahmad et al. (2019) reported the photocatalyst activity of polyaniline/Ni/Cellulose photocatalyst and PL intensity of Polyaniline/Ni/Cellulose is less than as compared to polyaniline/Ni and Polyaniline shows better performance of Polyaniline/Ni/Cellulose photocatalyst as shown in Fig. 4.

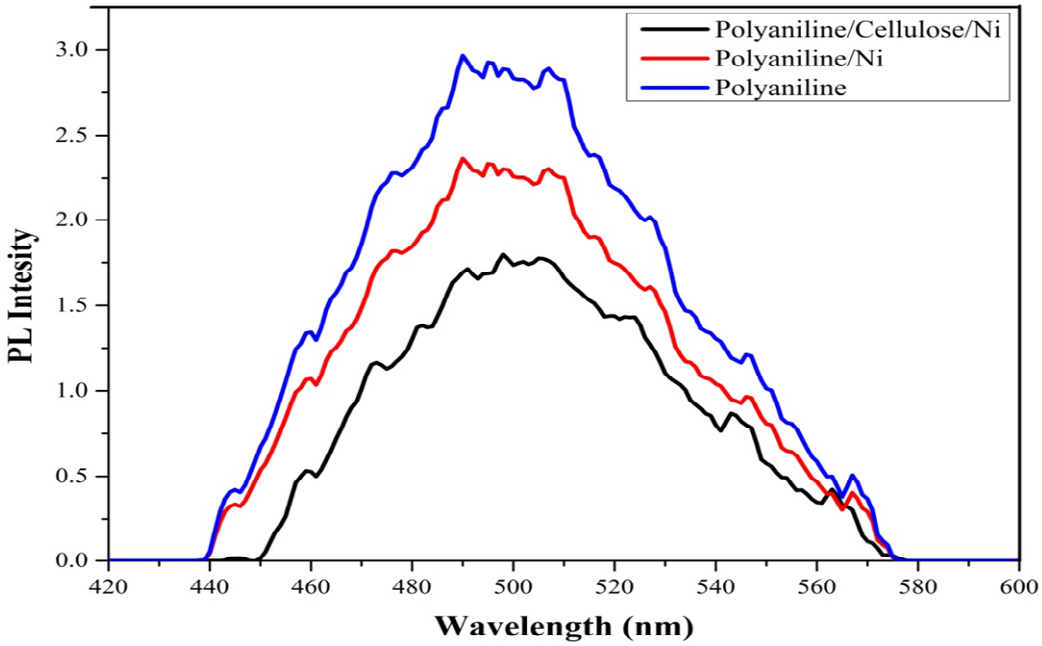

Fig.4:PL intensity of polyaniline and its composites (Ahmad et al. 2019)

Other way to avoid the recombination of electron-hole pairs and achieve maximum efficiency is to form heterojunction. Heterojunction can be formed either by the coupling of two different matrices with corresponding band potentials or through the capping of the nanocomposites. In the nanocomposites with the coupling, there is the interfacial charge transfer of the electrons and holes for reduction and oxidation on the surface of the nanocomposites. However, in the case of capped nanocomposites, the mechanism is a little bit different due to the presence of the core shell geometry where the electrons are transferred into the energy levels of the core semiconductor. In the case of the capped semiconductor, various properties of the nanocomposites such as photocatalytic, optical, and magnetic properties can be enhanced by altering parameters such as the shell thickness and the core radius (Pirzada et al. 2015). In the case of polymer nanocomposites, the heterojunction between the polymer and the nanoparticles are formed by coupling and transfer of charge carriers through interfacial contact (Kshirsagar et al. 2019, Wang et al. 2015, Bedja et al. 2002, Spanhel et al. 1991). A general representation of the heterogeneous photocatalysis of coupled and capped heterojunction are shown in Fig. S1 and S2 (Supplementary Information).

MOFs, COFs are also the most promising photocatalysts used for many applications and conducting polymer-MOFs and COFs nanocomposites can also be used for the treatment of wastewater while information on their use remains scarce to date.

3.2 Polymer-semiconductor nanocomposites

Semiconductor nanoparticles doped with the polymer as supporting matrix can act as promising photocatalyst for the photodegradation of organic pollutants. A number of researches based on polymer nanocomposites as photocatalyst are under progress for the treatment of wastewater and few recent examples are provided in Table 4. Semiconductor nanoparticles are found of much interest due to their enhanced properties in comparison to bulk counterparts such as larger surface area, reactive sites and light absorption capacity. In polymer-nanocomposites, semiconductor nanoparticles are doped with conducting polymer based on the suitable edge band potential of the conduction band and valence band so that photogenerated electron and holes can easily transfer through interfacial contact. Visible light active nanoparticles upon the irradiation generate reactive oxygen species and it also assists to suppress the recombination rate of photogenerated electrons and holes of the polymer.

3.2.1 Heterojunction (p-n, p-p, n-n type) mechanism

In the context of polymer, polyaniline, polypyrrole and polythiophene are the most investigated conducting polymer as photocatalyst due to their higher efficiency. The conducting polymers based on the mobility of their charge carriers are classified either as p-type or n-type. The conducting polymers (polyaniline, polypyrrole, polythiophene) are classified as p-type semiconductor as they are electron rich and conduct holes. In contrast, n-type conducting polymers can be formed through the partial reduction of these polymers, but the unstable nature of these n-type conducting polymers is an issue for their applications. The p-type conducting polymers can be formed p-p type heterojunction by doping with p-type semiconductor (CuS, NiO, V_2O_5, $ZnFe_2O_4$) and p-n type heterojunction by doping with n-type semiconductors (ZnO, TiO_2, WO_3). The movement of photogenerated electrons and holes between the junctions is based on the alignment of CB and VB. There is other type of the

heterojunction (n-n type) which are also studied in the photocatalytic application. In n-n type heterojunction, both the dopant and the host matrices are n type semiconductor and the heterojunction can be designed on the basis of CB and VB potential for the movement of electrons and holes. In the heterojunction, two mechanistic pathways are followed for the degradation of pollutants based on the potential of the valence band. The mechanisms are based on the generation of reactive oxygen species (ROS) during the photocatalytic reaction which is confirmed by the trapping experiment using various scavengers. Upon the irradiation of light, polymer nanocomposites absorb visible light irradiation and get excited and eject electrons. These exciting photogenerated electrons are transferred from HOMO to LUMO of the polymer through π-π* transition (Zhai et al. 2004). Further, the energy level of the coupled nanoparticle is matched with a polymer to form a synergistic interaction between these two matrixes and the electrons from the polymer are easily transferred to the nanoparticle. The electrons in the conduction band and holes of the valence band are reacting with H_2O molecules and atmospheric O_2 to form ROS. The first mechanism is described by taking the example of polyaniline (polyaniline, polypyrrole and polythiophene follow the same mechanism) which is based on the potential of the E_{VB} and E_{CB} of polyaniline. The E_{VB} and E_{CB} of polyaniline are 2.1 and -0.8 eV and E_{VB} of PANI do not have sufficient potential to oxide H_2O molecule into H^+ and ·OH- radicals. Therefore, polyaniline doped with the semiconductor nanoparticles such as Polyaniline-TiO_2 and polyaniline-ZnO which have E_{VB}> 2.7eV, so it can directly oxidize H_2O molecules to ·OH- radicals and follows the mechanism shown below (Equation 7-8).

$$O_2 + e^- \rightarrow {}^{\cdot}O_2^- \qquad (7)$$

$$H_2O + h^+ (VB) \rightarrow {}^{\cdot}OH + H^+ \qquad (8)$$

The second mechanism when the polyaniline is doped with the semiconductor nanoparticles which have the E_{VB} < 2.7eV such as Polyaniline-CdS, Polaniline-g-C_3N_4, Polyaniline-Cr_3O_4 and Polyaniline-Nickel ferrite. Here, H_2O molecules react with ${}^{\cdot}O_2^-$radical and form ${}^{\cdot}OOH$ and OH^- radicals which subsequently react with H_2O to generate ${}^{\cdot}OH$ radical and H_2O_2.

Further, based on alignments of CB and VB potentials in the heterojunction, three types of heterojunctions (type I, type II and type III) are generally designed for the photocatalysis mechanism as shown in Fig. 5 (Moniz et al. 2015, Zhu et al. 2019). In Type-I heterojunction, the alignments of both CB and VB of one matrix (A) is at higher potential than B so that the electrons and holes will be transferred from A to B. In such case, the chances of higher recombination of photogenerated electron and hole pairs are high because the transfer of electron and holes is happening to B only.

Type II heterojunction is used to design the photocatalytic mechanism of polymer nanocomposites (Ahmad et al. 2019, Ahmad et al. 2020). In type-II heterojunction, the alignments of CB show higher negative potential that nanoparticles and the alignment of VB is at lower positive potential than nanoparticles. The photoinduced holes and electrons can be transferred in the opposite direction to the enhanced the charge separation and suppress the recombination of electrons and holes thus enhance the photocatalytic performance. In type-III heterojunction, the alignments of both CB and VB of A and B is similar to type II but the difference of potentials are quite high which requires higher driving forces to transfer of photogenerated electrons and holes.

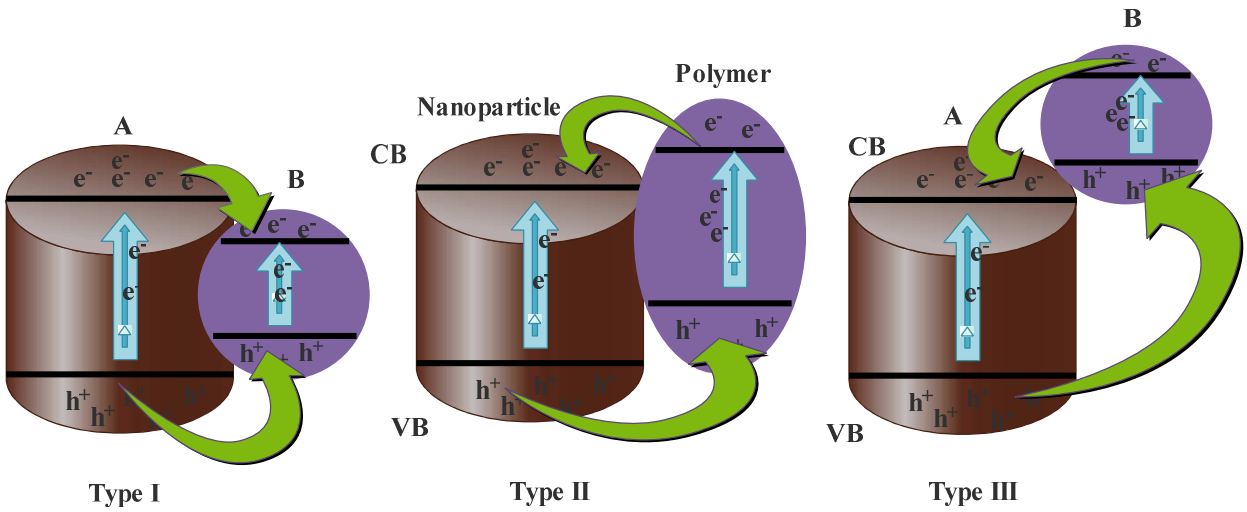

Fig. 5: Types of heterojunction of composites based on band alignment

3.2.2 Z-scheme photocatalysis by conducting polymers

Nanoparticles as well as conducting polymers such as polyaniline, polypyrrole and polythiophene follow Z-scheme photocatalytic degradation (Yang et al. 2021, Xie et al. 2020, Li et al. 2019,

Koutavarapu et al. 2021).A Z-scheme mechanism of conducting polymer and nanoparticle are shown in Fig. 6.

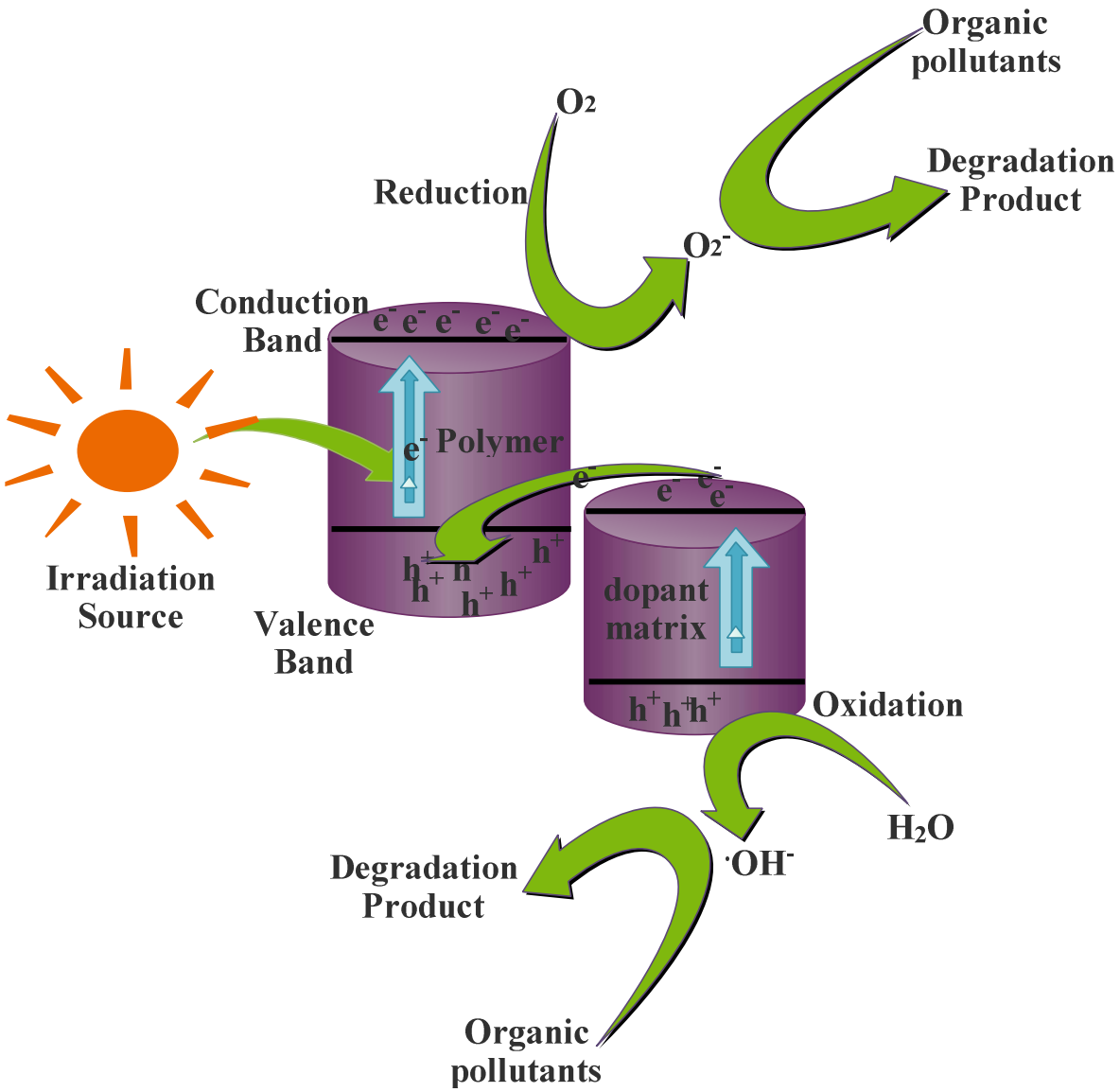

Fig. 6: Z-scheme mechanism of photocatalytic degradation of organic pollutants

In the Z-scheme mechanism, the alignment of fermi level of the conduction band of host matrix is very close to the valence band of the polymer matrix so that the electrons form a conduction band easing the transfer to the valence band and neutralizing the photogenerated holes. The electrons in the polymer matrix then reduce the O_2 to $\cdot O_2^-$radical, and holes in the valence band of host matrix oxides the H_2O molecules to (·OH) hydroxyl radicals.

3.3 Polymer-Graphene and Multiwall Carbon Nanotube (MWCNT) composites

Graphene and its derivatives are highly catalytic materials known as a reservoir of electrons (Zhang et al. 2016). Graphene has excellent properties such as higher surface area than most of the nanoparticles (Gadipelli et al. 2015) and electrical conductivity and processing. Graphene and its derivatives can be doped with conducting polymers to form polymer graphene composites. During the photocatalytic reaction, the electrons in the conduction band of the conducting polymer can easily transfer to the graphene and lower the recombination rate of electron and holes. Also, graphene has a much lower potential than polyaniline, polypyrrole and polythiophene, thus the interfacial charge transfer is feasible (Alam et al. 2018). Interaction through the π-π bond between delocalized electrons of graphene molecules and conducting polymer enhanced the properties of composites. MWCNTs also play a major role in the mechanism of photodegradation of pollutants with its interaction with nanoparticles or polymers. Recently Khan et al. (2020) synthesized MWCNT supported polypyrrole for the removal of Ponceau-BS dye in which MWCNT play an important role in the interfacial charge transfer. Other polymer nanocomposites such as polyaniline-rGO (reduced graphene oxide) (Mitra et a. 2019), polypyrrole/CdS-rGO (Ahmad et al. 2020), polyaniline-SWCNT (Chatterjee et al. 2017) have been used for the removal of organic pollutants. Graphene and MWCNTs molecules also assist in the adsorption of the organic pollutants on its surface and its adsorption efficiency can be increased through the addition of surfactant to graphene compound. In the photocatalytic mechanism electron from the conduction band can easily be transferred to the graphene sheet suppress the recombination of electron and hole pairs as shown in Fig. 7 and reactions (9-15) are shown below. Examples of various conducting polymer-biopolymer nanocomposites as photocatalyst are shown in Table S1.

$$\text{Polymer} + \text{rGO} + h\upsilon \rightarrow \text{Polymer} + \text{rGO}\,(h^+, e^-) \quad (9)$$

$$\text{Polymer}\,(e^-) + O_2 \rightarrow \cdot O_2^- \quad (10)$$

$$H_2O + \cdot O_2^- \rightarrow \cdot OOH + OH^- \quad (11)$$

$$\cdot OOH + H_2O \rightarrow \cdot OH + H_2O_2 \quad (12)$$

$$H_2O_2 + h^+ \rightarrow \cdot OOH + H^+ \quad (13)$$

$$H_2O_2 + \cdot OOH \rightarrow \cdot OH + H_2O + O_2 \quad (14)$$

$$\cdot O_2^-/\cdot OH/\ h^+ + \text{pollutants} \rightarrow \text{Degradation products} \quad (15)$$

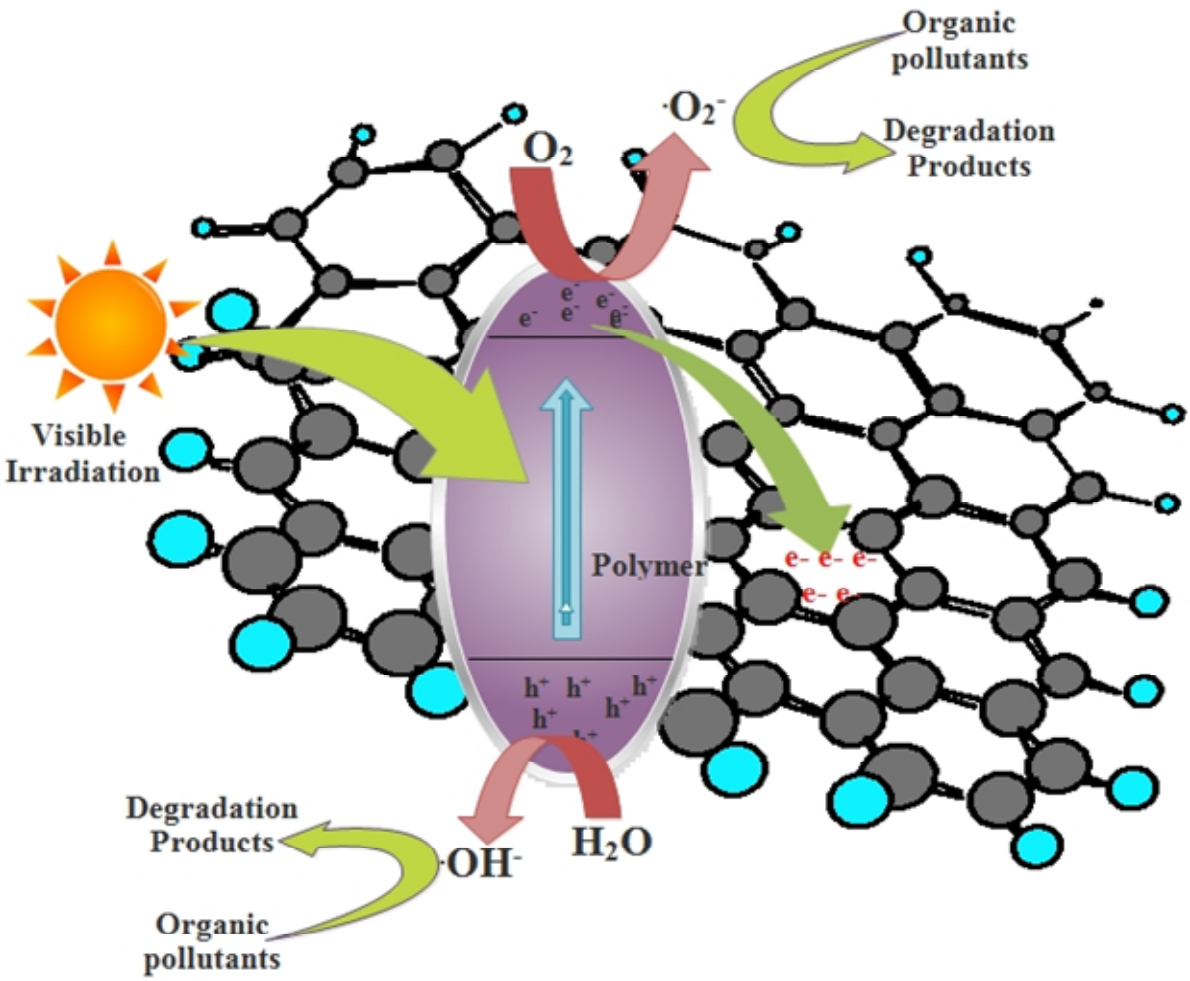

Fig. 7: Photocatalytic mechanism of polymer doped with graphene

3.4 Conducting polymer-biopolymer composites

Research work based on the conducting polymer-biopolymer composites as photocatalyst for the treatment of wastewater are limited to date. Biopolymer such as chitosan, chitin, cellulose, gelatine coupled with conducting polymers in the form of binary or ternary composites have been frequently used as photocatalyst for the treatment of wastewater. The formation of ROS is due to conducting polymer and the biopolymer helps in the adsorption of pollutants on its surface. These biopolymers

are not only assisting in the adsorption of pollutants to the photocatalyst but also act as a carrier of the nanoparticle in the photocatalytic mechanism. Chitosan is a cationic and hydrophilic polysaccharide, semi-crystalline in nature can be obtained by N-deacetylation of chitin, composed of β-D-glucosamine and acyl β-D-glucosamine residues with a 1,4-β-linkage (Younes et al. 2015). Chitosan is pH sensitive due to presence of NH_2 groups which get protonated in acidic medium (NH_3^+) and formed strong interaction between the anionic parts (SO_3^-) of the many toxic dyes. Ahmad et al. (2020) degraded Reactive Orange-16(RO-16) dye by polypyrrole/chitosan/ZnO bio-nanocomposites in which chitosan play a major role in the degradation of RO-16 dye with the interaction of NH_3^+ of chitosan and SO_3^- of RO-16 dye. Also, the presence of functional groups like NH_2 and OH provide the chelation ability with the functional group of the pollutants such as protonated NH_2 groups are capable of bonding with the SO_3^- groups of many organic dyes (Wang et al. 2007, Adnan et al. 2020).Conducting polymer-chitosan composite shave the ability to degrade number of pollutants such as toxic metals, micro pollutants, PAHs, PPCPs and organic dyes (Nagh et al. 2011, Kumar et al. 2020). A mechanism of conducting polymer/chitosan for the photodegradation of pollutant is shown in Fig. 8 and reactions (16-23) of photodegradation process are summarized below.

$$\text{Conducting polymer + biopolymer + } h\upsilon \rightarrow \text{Polymer } (h+, e-) \quad (16)$$

$$\text{Biopolymer + Pollutants} \rightarrow \text{Biopolymer-pollutants (Adsorption)} \quad (17)$$

$$\text{Polymer } (e-) + O_2 \rightarrow \cdot O_2^- \quad (18)$$

$$H_2O + \cdot O_2^- \rightarrow \cdot OOH + OH^- \quad (19)$$

$$\cdot OOH + H_2O \rightarrow \cdot OH + H_2O_2 \quad (20)$$

$$H_2O_2 + h^+ \rightarrow \cdot OOH + H^+ \quad (21)$$

$$H_2O_2 + \cdot OOH \rightarrow \cdot OH + H_2O + O_2 \quad (22)$$

$$\cdot O_2^- / \cdot OH / h^+ + \text{pollutants} \rightarrow \text{Degradation products} \quad (23)$$

Another biodegradable polymer, cellulose in its several forms such as bacterial cellulose (BC), cellulose nano-whiskers, and cellulose microfibres are used for the photocatalytic purpose. Bacterial

cellulose is a three- the adsorption of the pollutants on its surface (Mao et al. 2019). A study was conducted by Ahmad et al. 2017 of polypyrrole/cellulose/graphene oxide for the photodegradation of rhodamine B dye. Various conducting polymer-biopolymer nanocomposites as photocatalyst are shown in Table S2.

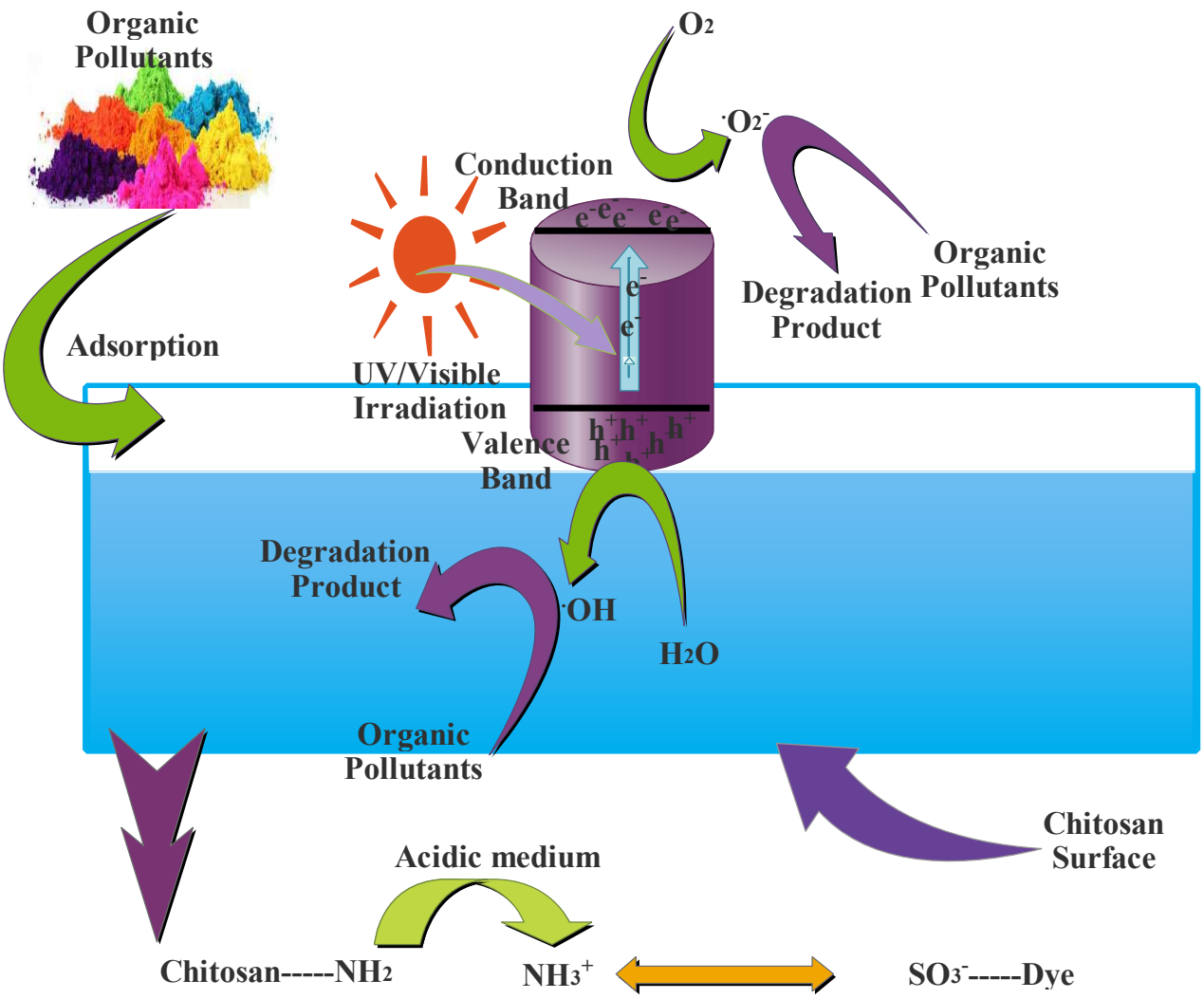

Fig. 8: Photocatalytic mechanism of polymer-biopolymer composites

3.5 Polymer- Clay nanocomposites (PCNs)

Polymer-Clay nanocomposites can be used for the wastewater treatment such as membrane technology and coagulants column treatment (Ginos et al. 2006, Mukhopadhyay et al. 2020). Polymer-clay nanocomposites such as polyurethane-clay, epoxy-clay, polyimide-clay, organoclay-polymer, biopolymer-clay, and magnetic clay-polymer have been used as an adsorbent for the

removal of wastewater contaminants (Mukhopadhyay et al. 2020). Polymers such as polyaniline, polypropylene, polystyrene, polyurethane are used to form polymer clay composites in which the clay acts as supporting matrix. Natural clay with its excellent properties such as high adsorption capability, specific surfaces areas, large pore volumes can be used as supporting material as fillers in the composites (Dong et al. 2012, Mishra et al. 2018). These types of photocatalysts are able to degrade wide range of pollutants such as toxic metals, micro pollutants, PAHs, PPCPs, volatile organic compounds and organic dyes (Mishra et al. 2017). Clays such as sepiolite (Naing et al. 2020), imogolite (Irie et al. 2008), halloysite Papoulis et al. 2013), kaolinite (Zhang et al. 2011) and bentonite (Mishra et al. 2018) are the examples of the catalysts which show the excellent activity towards the degradation of pollutants. A mechanism of conducting polymer-Clay composites is shown in Fig. 9 and reaction (24-31) are shown below.

$$\text{Conducting polymer} + \text{Clay} + h\upsilon \rightarrow \text{Polymer } (h+, e-) \quad (24)$$

$$\text{Clay} + \text{Pollutants} \rightarrow \text{Clay-pollutants (Adsorption)} \quad (25)$$

$$\text{Polymer } (e-) + O_2 \rightarrow \cdot O_2^- \quad (26)$$

$$H_2O + \cdot O_2^- \rightarrow \cdot OOH + OH^- \quad (27)$$

$$\cdot OOH + H_2O \rightarrow \cdot OH + H_2O_2 \quad (28)$$

$$H_2O_2 + h^+ \rightarrow \cdot OOH + H^+(^+ \quad (29)$$

$$H_2O_2 + \cdot OOH \rightarrow \cdot OH + H_2O + O_2 \quad (30)$$

$$\cdot O_2^- / \cdot OH / h^+ + \text{pollutants} \rightarrow \text{Degradation products} \quad (31)$$

Few factors affect the adsorption of contaminants on the polymer clay nanocomposites such as surface area, functional groups, surface charge, pH, temperature, the concentration of the pollutants. Clay can have either cationic or anionic surface charge that helps in the interactions between contaminants and polymer clay composites such as electron donor-acceptor interaction, electrostatic attraction, hydrogen bonding and ion-exchange to remove the contaminants from wastewater(Mukhopadhyay et al. 2020).Clay has been used as excellent support with many

nanoparticles such as graphene oxide (Gogoi et al. 2019), ZnO, TiO_2 (Szczepanik, 2017), SnO_2 (Babu et al. 2019) for the photocatalytic degradation of organic pollutants. However, literature is still scarce on conducting polymer clay composite for photocatalysis purposes.

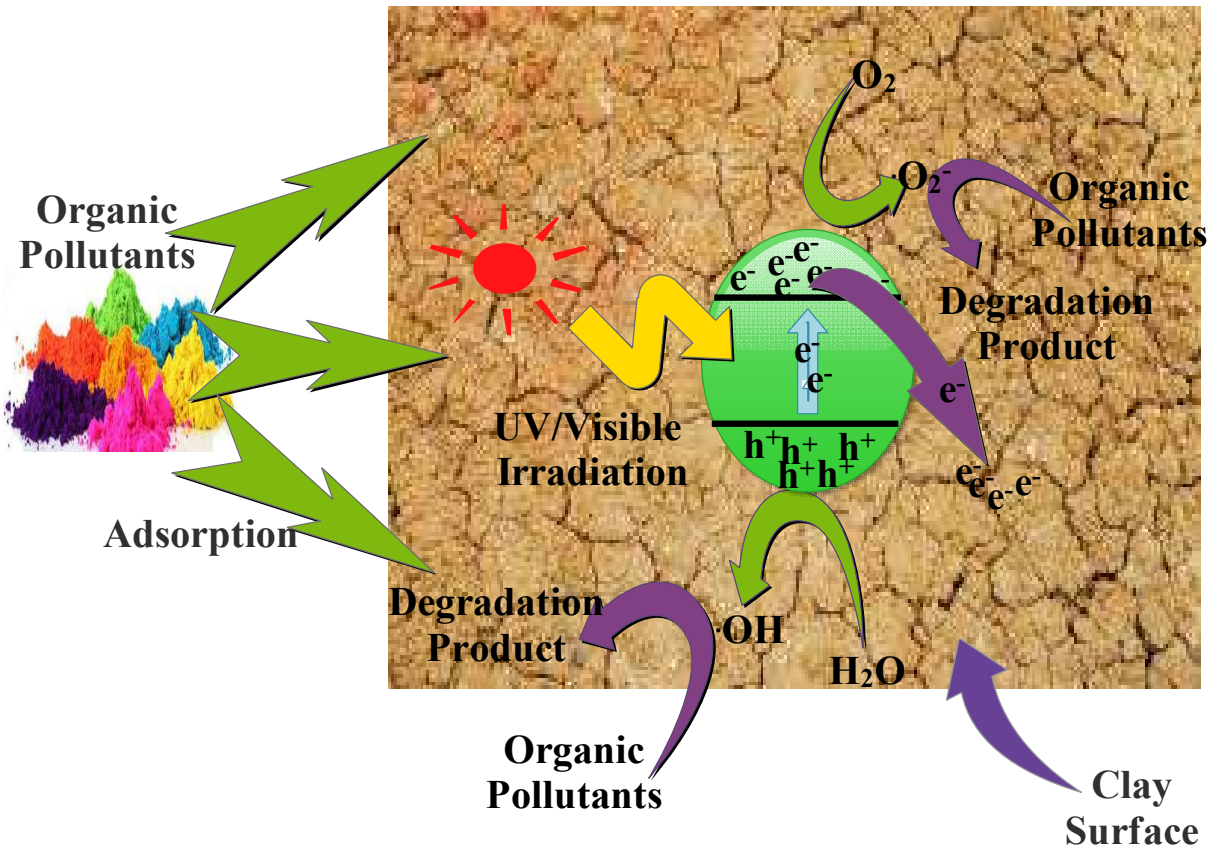

Fig. 9: Photocatalytic mechanism of polymer-clay composites

4 Factors affecting the photocatalytic degradation of organic pollutants in wastewater

There are many factors which significantly affect the photocatalytic activity of the photocatalysts. A concise summary of these factors is presented in Table 4 and the detailed information is discussed below.

Table 4: Summary of the factors and their effect on the photocatalytic degradation

S.No.	Factors	Effect on photodegradation
1	Effect of photocatalyst amount	Photocatalytic activity improves with increase the amount of dopant up to certain limit and then decreases.
2	Size and morphology of photocatalyst	Size less than 100 nm is quite effective in photodegradation as it enhances the surface to volume ratio and different shapes of nanoparticles such as nanorods, nanotubes have different photocatalytic activity.

3	Surface area	Surface area is directly proportional to the photocatalytic activity as it increases the number of active sites on the photocatalyst surface that binds to the pollutants.
4	Reaction temperature	The ideal temperature to operate photocatalytic experiment should be in the range of 20-80 °C.
5	Concentration and nature of organic pollutants	Higher concentration of the pollutants leads to the reduction of photocatalytic activity as a portion of irradiation are absorbed by the pollutants and less photogenerated electrons and holes are produced. Various functional groups (electron donating and electron accepting groups) also affect the photocatalytic activity.
6	Effect of pH	pH value of the pollutants is directly interlinked with the surface charge of the photocatalyst and helps in the producing H^+ and Hydroxide radicals.
7	Inorganic ions present in the water	Various inorganic ions such as chloride, nitrates, carbonates and sulphates affect the photocatalytic activity.
8	Effect of dopant	Dopant helps in suppressing the recombination of photogenerated of electrons and holes thus increases the photocatalytic activity.
9	Effects of light intensity, wavelength and the irradiation time	Photocatalyst with different band gap energy requires different wavelength of the irradiation (UV or visible irradiation). Irradiation time also affects the photocatalytic activity. Photocatalyst that degrade the pollutants in less time is most effective photocatalyst.

4.1 Effect of photocatalyst amount

The photodegradation process is significantly affected by the amount of photocatalyst (Ajmal et al. 2014, Gouvea et al. 2000, Saquib et al. 2002). If the amount of photocatalyst is increased during the photocatalysis process, then the numbers of active sites available to bind with pollutants molecules are also increased. In the case of heterogeneous photocatalysts, an increase in the amount of dopant material favours higher activity because the photogenerated electrons are transferred at the interface of the dopant and the host material which suppress the recombination rate of photogenerated electron and holes. However, adding too much catalyst can retard or suppress the photocatalysis efficiency because the aqueous solution of pollutants and the photocatalyst become turbid which blocks the irradiation and inhibits the photocatalytic reaction (Colemn et al. 2007, Kumar et al. 2015, Kumar et al. 2017).

4.2 Size and morphology of the photocatalyst

Size and structure of the photocatalyst show significant effect in the photodegradation mechanism. The size of the photocatalyst in nano range (less than 100 nm) increases its surface to volume ratio and can effectively interact to dye molecules. Surface morphology (i.e. the structure of the

photocatalyst) has a direct connection in the photocatalysis mechanism in bonding between catalyst and pollutants (Zhu et al. 2006). For example, goethite particles in the form of short rod- pancake and long rod-like was studied and the particle with a short rod and pancake-like particles have higher photocatalytic activity owing to higher surface area (Kakuta et al. 2014). Mogyorosi et al. (2010) studied various polyhedral TiO_2 particles with varying surface area and the particles P25 B TiO_2 with the higher surface area had the higher photocatalytic activity toward phenol decomposition

4.3 Surface area

Surface area finds an important role in photocatalytic reaction to achieve the maximum efficiency as the chemical reactions take place at the surface of the photocatalyst (Ameen et al. 2012). In this case, interaction and adsorption of various catalysts play an important role in the reaction. The surface area of polymer nanocomposite can be increased by doping the nanostructure materials to the polymers. Doping may result in both increasing and decreasing of the resultant synthesized photocatalysts. If the surface of the host material is smooth, then there is the probability of increasing surface area of the resultant material but if the surface of the host material is in the porous form then that dopant can be settling down into that pores and in this case the surface area may be decreased. The photocatalyst with the higher surface area has a greater number of reactive species available to bind with the pollutants. Ahmad et al. (2017) reported the effect of surface area on the photocatalysis by comparing the surface area and photocatalytic activity of polyaniline, polyaniline/Ni and polyaniline/Ni/Cellulose. The higher surface area of Polyaniline/Ni/Cellulose favours higher activity as compare the other two photocatalysts.

4.4 Reaction temperature

The reaction temperature of the photochemical reactor equipped with visible or UV light irradiation affects the rate of photodegradation (Soares et al. 2007, Reza et al. 2017). An increase in the temperature at a certain level favours higher photocatalytic activity. The desired reaction temperature of the photochemical reactor should be in the range of 20-80 ˚C which is the optimum temperature condition for the photocatalysis. The temperature above 80 ˚C may result in higher recombination

rate of photogenerated electron and holes pairs and also disfavours the adsorption of dyes on the photocatalyst surface (Hashimoto et al. 2005). Adsorption also plays an important role in the interaction and bonding between dye and photocatalyst. However, the temperature below 20 ˚C may lead to a decrease in the apparent activation energy of photocatalyst which is essential for the activation of the photocatalyst so the temperature below 20 ˚C is not favourable for photocatalysis (Mamba et al. 2014).

4.5 Concentration and nature of organic pollutants

The photocatalytic efficiency of catalyst depends upon concentration and the nature of photocatalyst. The higher concentration of the dye molecules reduces the photonic efficiency of the photocatalyst because the higher concentration of the dye inhibits the irradiation and subsequently lowers the efficiency. Various research groups have worked on the degradation of different dyes such as Gentian Violet with various concentration 73.4, 101.9, 142.7 and 203 mg/l, however the concentration higher than 100 mg/l disfavours the photocatalytic activity (Saquib et al. 2003). Another study of the Acid Orange-7 dye was conducted between 25-600 mg/l and the same results was found to the concentration of 25-100 mg/l while the concentration above the 200-600 mg/l was not favourable (Kiriakodou et al. 1999). Other groups studied various dyes at different concentration like Reactive Yellow-150 in range of 0.02 to 0.1 mg/l with a fixed amount of photocatalysts and it has been noted that the percentage degradation of the dye decreased when increasing the concentration of dye (Illinous et al. 2013). These findings suggested that as the dye concentration increase, the molecules of dye are adsorbed on the surface of the photocatalyst which inhibits the penetration of irradiation source and therefore inhibit reaction. Another factor is the nature of pollutants is the substituent groups present on the pollutants i.e. substrate with electron-withdrawing nature like nitrobenzene, benzoic acid, phenol have strong tendency to adhere to photocatalyst and are more liable to mineralization (Tian et al. 2009).

4.6 Effect of pH

The photocatalysis consists of three different parts of reactions mechanism in which the formation and contribution of the hydroxyl radicals, oxidation by the positive holes and reduction by the photogenerated electrons and these factors are interlinked with pH (Reza et al. 2017). The pH value of the solution helps to separate the photogenerated electron and the holes pairs. It has been found in some study that pH factor is linked with the nature of the dye (cationic or anionic) and the surface charge of the photocatalyst. Generally, cationic dye with lower pH favours the higher degradation of dye although in case of the degradation of methylene blue by TiO_2 favours the higher pH due to basic pH electrostatic between negative TiO^- and methylene blue cation forms strong interaction which results in higher photodegradation (Ling et al. 2004). Baran et al. (2008) observed the dominance of acidic pH in the degradation of bromocresol purple but the activity can be increased to a certain level. In the higher acidic condition i.e. less than 5 the presence of a higher concentration of proton in the solution lowers the efficiency (Baran et al. 2008). Conversely, in the higher basic medium, the presence of $^{\cdot}OH$ ion neutralizes the acidic end product resulted from photodegradation reaction. Chromophores and the substituents also depend on the variation of the pH of the solution. Anionic dye with the positive charge groups favours the basic medium for the better photocatalytic activity. Various groups present on the dye molecules such as Cl^-, SO_3^- favours the acidic medium for better activity (Hind et al. 2002).

4.7 Inorganic ions present in the water

The wastewater contains various ions both cation and anion such as magnesium, calcium, copper, zinc, chloride, nitrate, sulphate and carbonates (Rauf et al. 2009, Liao et al. 2001, Wang et al. 2011)and the presences of these ions in the water is of great obstacle in the photocatalytic process. These ions tend to form strong bonding with the photocatalyst. Cations such as Fe^{2+} and Cu^{2+} and anions such as phosphate, nitrates, chlorides and sulphates significantly retard the photodegradation process, while the presence of Mg^{2+}, Zn^{2+}, Ca^{2+} have a minor effect. The wastewater that contains salt reduces the colloidal stability of the solution and decrease the interfacial contact between

photocatalyst and the dyes. The presence of the carbonates and chloride ions in the water also works as the trapping agents of the ˙OH and h^+ thus retards the photocatalytic activity as shown in equation (32-37) (Iguchi et al. 2015).

$$CO_3^{2-} + OH^{\cdot} \rightarrow CO_3^{-\cdot} + OH^{-}(^{-} \quad (32)$$

$$HCO_3^{-} + OH^{\cdot} \rightarrow CO_3^{-\cdot} + H_2O \quad (33)$$

$$CO_3^{-\cdot} + OH^{\cdot} \rightarrow HCO_3^{-} \quad (34)$$

$$Cl^{-} + h+(VB) \rightarrow Cl^{\cdot} \quad (35)$$

$$OH^{\cdot} + Cl^{-} \rightarrow HOCl^{-\cdot} \quad (36)$$

$$HOCl^{-\cdot} + H^{+} \rightarrow Cl^{\cdot} + H_2O \quad (37)$$

However, in some study, it has been reported that the presence of some ions such as NO_3^- and SO_4^{2-} enhances the photocatalytic activity (Zhu et al. 2005, Wang et al. 2011). NO_3^- upon reaction with H_2O in the presence of light creates $OH^{\cdot}$ which plays an important role in the photodegradation and Sulphate ions SO_4^{2-} when react with photogenerated holes it prevents the recombination of photogenerated electrons to holes.

4.8 Effect of dopant

For a higher photocatalytic, doping of the photocatalyst is of utmost importance. The dopant plays a vital role in the photodegradation mechanism through surface modification and reduction of the band gap as well. The doping material (dopant) assists the catalyst in the electron transfer via interfacial charge transfer of Schottky barrier or transfer of an electron to other particles (Mehraj et al. 2015). In order to suppress the recombination rate of the photocatalyst doping is done. One other parameter that affects in doping of cation and anion is the shifting of the fermi level of the host material, so the band gap decreased in the resultant photocatalyst. Sometimes the band gap of certain photocatalyst lies in the UV-region which subsequently changes to the visible region after the doping process and the transfer of electron can easily be transferred from the valence band to the conduction band. The process of shifting the band gap is known as the bathochromic shift. A wide range of the

photocatalytic studies found that the efficiency increased upon doping of composites rather thana single catalyst. Such as TiO_2, which is the most promising photocatalyst for the degradation of the dyes has been doped by various metal ions like Ni^+, Zn^+, Cu^+, Fe^{3+} etc because of the major drawback of the TiO_2 that the band gap energy lies in the UV region (Yu et al. 2002, Chong et al. 2010).

4.9 Effect of light intensity, wavelength, and the irradiation time

For the different range of the photocatalysts (i.e. visible range and UV range photocatalyst) different irradiation sources are used. Photocatalyst with the band gap energy higher that >3eV (wavelength < 400 nm) are supposed to irradiate under the influence of the UV light and the catalyst with the band gap energy less than <3eV (<400 nm) are irradiated under the visible light (Stylidi et al. 2004). Solar energy due to its ease availability and non-hazardous nature is the most effective source of the irradiation in photocatalysis. The wavelength of the solar irradiation reaching to the earth is >340 nm that contains only a little portion of UV light. The UV light range is 200-400 nm which has the higher energy and has significant effect of the photodegradation while the visible light range is 400-800 nm is the most suitable for the photocatalyst with lower band gap energy under sun light. Light of the lower wavelength with high energy helps in more effectively for the photocatalysis. These two factors, wavelength and energy are inversely proportional to each other.

The photodegradation mechanism depends on the three factors of intensities of the light. At the lower intensities of the light, the rate would increase linearly with increasing light intensity (first-order) and at the intermediate light intensities, the rate would depend on the square root of the light intensities (half order) and at the higher intensities rate of photodegradation is independent of light intensity due to generation of more photons which attracts on the catalyst surface while the number of the active site on the catalyst is same but the intensity of the light increasing constantly. At higher intensity, the formation of electron-hole pairs is high and there is very less chance of the recombination of these electron-hole pairs. However, in the case of lower intensities, there is less generation of electron-hole pairs and a higher chance of recombination (Ollis et al. 1992). So, it can be concluded that the higher intensities favour the higher photocatalysis efficiency. Moreover, the photocatalyst that can degrade

the pollutants in less time is considered to be more effective because according to the -pseudo-first-order kinetic the rate of the reaction decreased with irradiation time. However, in some cases the photocatalytic efficiency increases with increase in irradiation time of photodegradation reaction.

5 Conclusions and Future Perspectives

The review provides inclusive information about the photocatalysis and its mechanism for treatment of wastewater. Photocatalytic methods are preferred over chemical, physical, and biological methods for the degradation of the major organic chemical pollutants. The photocatalytic degradation of organic pollutants has been found quite efficient with maximum efficiency and complete degradation of pollutants to harmless products. However, there are certain drawbacks associated with photocatalysis, but they can be overcome by combining it with the biological processes that are capable to degrade the pollutant completely. The composite of conducting polymers with semiconductor nanoparticles, graphene, MWCNT and biodegradable polymer are promising photocatalysts in term of efficient formation of reactive oxygen species and lower recombination of electrons and holes. Conducting polymer with clay and biopolymer are showing higher efficiency due to their excellent adsorption property and characteristics functional groups. These conducting polymer nanocomposites can also be applied for a wide range of pollutants apart from those discussed in this review. Thus, in the light of their catalytic activity, stability, and reusability, polymer-based nanocomposites make photocatalytic treatment more competitive and effective for the removal of contaminants from wastewater. However, understanding the effect or wastewater matrices is needed as it will help in developing novel photocatalytic strategies for field application and inform operational requirement such as electricity consumption, recovery of the photocatalysts and cost consumption for the photocatalytic process.

Acknowledgements

Nafees Ahmad is grateful for the PhD Split-site scholarship award by the Commonwealth Scholarship Commission United Kingdom (Award number INCN-2019-35).

Declaration of Competing Interest

There are no conflicts of interest to declare

References

Abinaya, M., Rajakumaran, R., Chen, S. M., Karthik, R., & Muthuraj, V. (2019). In Situ synthesis, characterization, and catalytic performance of polypyrrole polymer-incorporated Ag2MoO4 nanocomposite for detection and degradation of environmental pollutants and pharmaceutical drugs. ACS applied materials & interfaces, 11(41), 38321-38335.

Abramović, B., Despotović, V., Šojić, D., & Finčur, N. (2015). Mechanism of clomazone photocatalytic degradation: hydroxyl radical, electron and hole scavengers. Reaction Kinetics, Mechanisms and Catalysis, 115(1), 67-79.

Adegoke, K. A., & Bello, O. S. (2015). Dye sequestration using agricultural wastes as adsorbents. *Water Resources and Industry*,*12*, 8-24.

Adnan, M. A. M., Phoon, B. L., & Julkapli, N. M. (2020). Mitigation of pollutants by chitosan/metallic oxide photocatalyst: a review. *Journal of Cleaner Production*, 121190.

Ahmad, N., Sultana, S., Azam, A., Sabir, S., & Khan, M. Z. (2017). Novel bio-nanocomposite materials for enhanced biodegradability and photocatalytic activity. *New Journal of Chemistry*, *41*(18), 10198-10207.

Ahmad, N., Sultana, S., Faisal, S. M., Ahmed, A., Sabir, S., & Khan, M. Z. (2019). Zinc oxide-decorated polypyrrole/chitosan bionanocomposites with enhanced photocatalytic, antibacterial and anticancer performance. *RSC Advances*, 9(70), 41135-41150.

Ahmad, N., Sultana, S., Kumar, G., Zuhaib, M., Sabir, S., & Khan, M. Z. (2019). Polyaniline based hybrid bionanocomposites with enhanced visible light photocatalytic activity and antifungal activity. *Journal of Environmental Chemical Engineering*, *7*(1), 102804.

Ahmad, N., Sultana, S., Sabir, S., & Khan, M. Z. (2020). Exploring the visible light driven photocatalysis by reduced graphene oxide supported Ppy/CdS nanocomposites for the

degradation of organic pollutants. *Journal of Photochemistry and Photobiology A: Chemistry*, *386*, 112129.

Ajmal, A., Majeed, I., Malik, R. N., Idriss, H., & Nadeem, M. A. (2014). Principles and mechanisms of photocatalytic dye degradation on TiO 2 based photocatalysts: a comparative overview. *RSC Advances*, 4(70), 37003-37026.

Akhundi, A., Badiei, A., Ziarani, G. M., Habibi-Yangjeh, A., Muñoz-Batista, M. J., & Luque, R. (2020). Graphitic carbon nitride-based photocatalysts: toward efficient organic transformation for value-added chemicals production. *Molecular Catalysis*, 488, 110902.

Akhundi, A., Habibi-Yangjeh, A., Abitorabi, M., & Rahim Pouran, S. (2019). Review on photocatalytic conversion of carbon dioxide to value-added compounds and renewable fuels by graphitic carbon nitride-based photocatalysts. *Catalysis Reviews*, 61(4), 595-628.

Alam, U., Khan, A., Raza, W., Khan, A., Bahnemann, D., & Muneer, M. (2017). Highly efficient Y and V co-doped ZnO photocatalyst with enhanced dye sensitized visible light photocatalytic activity. *Catalysis Today*, 284, 169-178.

Aleboyeh, A., Kasiri, M. B., & Aleboyeh, H. (2012). Influence of dyeing auxiliaries on AB74 dye degradation by UV/H_2O_2process. *Journal of Environmental Management*, *113*, 426-431.

Ameen, S., Seo, H. K., Akhtar, M. S., & Shin, H. S. (2012). Novel graphene/polyaniline nanocomposites and its photocatalytic activity toward the degradation of rose Bengal dye. *Chemical Engineering Journal*,*210*, 220-228.

Anjum, M., Miandad, R., Waqas, M., Gehany, F., & Barakat, M. A. (2019). Remediation of wastewater using various nano-materials. *Arabian Journal of Chemistry*, 12(8), 4897-4919.

Asadzadeh-Khaneghah, S., & Habibi-Yangjeh, A. (2020). g-C3N4/carbon dot-based nanocomposites serve as efficacious photocatalysts for environmental purification and energy generation: A review. *Journal of Cleaner Production*, 124319.

Asgari, E., Esrafili, A., Jafari, A. J., Kalantary, R. R., Nourmoradi, H., & Farzadkia, M. (2019). The comparison of ZnO/polyaniline nanocomposite under UV and visible radiations for

decomposition of metronidazole: degradation rate, mechanism and mineralization. *Process Safety and Environmental Protection*, 128, 65-76.

Augugliaro, V., Baiocchi, C., Prevot, A. B., García-López, E., Loddo, V., Malato, S., ... & Pramauro, E. (2002). Azo-dyes photocatalytic degradation in aqueous suspension of TiO2 under solar irradiation. *Chemosphere*, 49(10), 1223-1230.

Ayappan, C., Jayaraman, V., Palanivel, B., Pandikumar, A., & Mani, A. (2020). Facile preparation of novel Sb2S3 nanoparticles/rod-like α-Ag_2WO_4 heterojunction photocatalysts: Continuous modulation of band structure towards the efficient removal of organic contaminants. *Separation and Purification Technology*, *236*, 116302.

Azami, M. S., Ismail, K., Ishak, M. A. M., Zuliahani, A., Hamzah, S. R., & Nawawi, W. I. (2020). Formation of an amorphous carbon nitride/titania composite for photocatalytic degradation of RR4 dye. *Journal of Water Process Engineering*, *35*, 101209.

Babu, A. T., & Antony, R. (2019). Clay semiconductor hetero-system of SnO_2/bentonite nanocomposites for catalytic degradation of toxic organic wastes. *Applied Clay Science*, 183, 105312.

Babu, B., Koutavarapu, R., Shim, J., Kim, J., & Yoo, K. (2021). Enhanced solar-light-driven photocatalytic and photoelectrochemical properties of zinc tungsten oxide nanorods anchored on bismuth tungsten oxide nanoflakes. *Chemosphere*, 268, 129346.

Bano, S., Ahmad, N., Sultana, S., Sabir, S., & Khan, M. Z. (2019). Preparation and study of ternary polypyrrole-tin oxide-chitin nanocomposites and their potential applications in visible light photocatalysis and sensors. *Journal of Environmental Chemical Engineering*, 7(2), 103012.

Baran, W., Makowski, A., &Wardas, W. (2008). The effect of UV radiation absorption of cationic and anionic dye solutions on their photocatalytic degradation in the presence TiO_2. *Dyes and Pigments*, *76*(1), 226-230.

Bedja, I., & Kamat, P. V. (2002). Capped semiconductor colloids. Synthesis and photoelectrochemical behavior of TiO_2-capped SnO_2nanocrystallites. *The Journal of Physical Chemistry*, *99*(22), 9182-9188.

Bizani, E., Fytianos, K., Poulios, I., & Tsiridis, V. (2006). Photocatalytic decolorization and degradation of dye solutions and wastewaters in the presence of titanium dioxide. *Journal of Hazardous Materials,* 136(1), 85-94.

Bolisetty, S., Peydayesh, M., & Mezzenga, R. (2019). Sustainable technologies for water purification from heavy metals: review and analysis. *Chemical Society Reviews*, 48(2), 463-487.

Boruah, P. K., & Das, M. R. (2020). Dual responsive magnetic Fe_3O_4-TiO_2/graphene nanocomposite as an artificial nanozyme for the colorimetric detection and photodegradation of pesticide in an aqueous medium. *Journal of Hazardous Materials*, *385*, 121516.

Chatterjee, M. J., Ghosh, A., Mondal, A., & Banerjee, D. (2017). Polyaniline–single walled carbon nanotube composite–a photocatalyst to degrade rose Bengal and methyl orange dyes under visible-light illumination. *RSC advances*, *7*(58), 36403-36415.

Cheng, X., Shang, Y., Cui, Y., Shi, R., Zhu, Y., & Yang, P. (2020). Enhanced photoelectrochemical and photocatalytic properties of anatase-TiO_2 (B) nanobelts decorated with CdS nanoparticles. *Solid State Sciences*, 99, 106075.

Chong, M. N., Jin, B., Chow, C. W., & Saint, C. (2010). Recent developments in photocatalytic water treatment technology: a review. *Water research*, *44*(10), 2997-3027.

Coleman, H. M., Vimonses, V., Leslie, G., & Amal, R. (2007). Degradation of 1, 4-dioxane in water using TiO_2 based photocatalytic and H_2O_2/UV processes. *Journal of Hazardous Materials*, *146*(3), 496-501.

Di Mauro, A., Cantarella, M., Nicotra, G., Pellegrino, G., Gulino, A., Brundo, M. V., ... & Impellizzeri, G. (2017). Novel synthesis of ZnO/PMMA nanocomposites for photocatalytic applications. *Scientific reports*, 7(1), 1-12.

Dong, Y., Liu, Z., & Chen, L. (2012). Removal of Zn (II) from aqueous solution by natural halloysite nanotubes. *Journal of Radioanalytical and Nuclear Chemistry*, *292*(1), 435-443.

Ebrahimi, R., Maleki, A., Zandsalimi, Y., Ghanbari, R., Shahmoradi, B., Rezaee, R., ...& Giahi, O. (2019). Photocatalytic degradation of organic dyes using WO_3-doped ZnO nanoparticles fixed on a glass surface in aqueous solution. *Journal of Industrial and Engineering Chemistry*, 73, 297-305.

Estrada, A. L., Li, Y. Y., & Wang, A. (2012). Biodegradability enhancement of wastewater containing cefalexin by means of the electro-Fenton oxidation process. *Journal of hazardous materials*, 227, 41-48.

Forgacs, E., Cserhati, T., & Oros, G. (2004). Removal of synthetic dyes from wastewaters: a review. *Environment international*, *30*(7), 953-971.

Gadipelli, S., & Guo, Z. X. (2015). Graphene-based materials: Synthesis and gas sorption, storage and separation. *Progress in Materials Science*, 69, 1-60.

Gao, B. Y., Hahn, H. H., & Hoffmann, E. (2002). Evaluation of aluminium-silicate polymer composite as a coagulant for water treatment. *Water Research*, 36(14), 3573-3581.

Gao, X., Liang, C., Gao, K., Li, X., Liu, J., & Li, Q. (2020). Z-scheme heterojunction Ag_3PO_4/$BiVO_4$ with exposing high-active facets and stretching spatial charge separation ability for photocatalytic organic pollutants degradation. *Applied Surface Science*, 146506.

Gaur, N., Narasimhulu, K., & Pydisetty, Y. (2018). Recent advances in the bioremediation of persistent organic pollutants and its effect on environment. *Journal of cleaner production*, 198, 1602-1631.

Geng, T., Chen, H., Xu, J., Ren, M., Liu, J., & Cao, F. (2019). Removal of nickels from crude oil to water by two micro-sized core-shell particles bearing poly (N-vinyl pyrrolidone). Fuel, 245, 181-187.

Ginos, A., Manios, T., & Mantzavinos, D. (2006). Treatment of olive mill effluents by coagulation–flocculation–hydrogen peroxide oxidation and effect on phytotoxicity. *Journal of hazardous materials*, 133(1-3), 135-142.

Gogoi, J., Choudhury, A. D., & Chowdhury, D. (2019). Graphene oxide clay nanocomposite as an efficient photo-catalyst for degradation of cationic dye. *Materials Chemistry and Physics*, *232*, 438-445.

Gómez-Pacheco, C. V., Sánchez-Polo, M., Rivera-Utrilla, J., & López-Peñalver, J. (2011). Tetracycline removal from waters by integrated technologies based on ozonation and biodegradation. *Chemical Engineering Journal*, 178, 115-121.

Gouvea, C. A., Wypych, F., Moraes, S. G., Duran, N., Nagata, N., &Peralta-Zamora, P. (2000). Semiconductor-assisted photocatalytic degradation of reactive dyes in aqueous solution. *Chemosphere*, *40*(4), 433-440.

Guo, J., Lee, J. G., Tan, T., Yeo, J., Wong, P. W., Ghaffour, N., & An, A. K. (2019). Enhanced ammonia recovery from wastewater by Nafion membrane with highly porous honeycomb nanostructure and its mechanism in membrane distillation. Journal of Membrane Science, 590, 117265.

Gupta, V. K. (2009). Application of low-cost adsorbents for dye removal–a review. *Journal of Environmental Management*, *90*(8), 2313-2342.

Habibi-Yangjeh, A., Asadzadeh-Khaneghah, S., Feizpoor, S., & Rouhi, A. (2020). Review on heterogeneous photocatalytic disinfection of waterborne, airborne, and foodborne viruses: Can we win against pathogenic viruses? Journal of Colloid and Interface Science. 580:503-514.

Hameed, B. H., Din, A. M., & Ahmad, A. L. (2007). Adsorption of methylene blue onto bamboo-based activated carbon: kinetics and equilibrium studies. *Journal of Hazardous Materials*, *141*(3), 819-825.

Hashimoto K., Irie H., & Fujishima A. 2005. TiO2 photocatalysis: A historical overview and future prospects. *Japanese Journal of Applied Physics*. 44:8269-8285

He, S., Wang, J., Ye, L., Zhang, Y., & Yu, J. (2014). Removal of diclofenac from surface water by electron beam irradiation combined with a biological aerated filter. *Radiation Physics and Chemistry*, 105, 104-108.

Hethnawi, A., Nassar, N. N., Manasrah, A. D., & Vitale, G. (2017). Polyethylenimine-functionalized pyroxene nanoparticles embedded on Diatomite for adsorptive removal of dye from textile wastewater in a fixed-bed column. *Chemical Engineering Journal*, *320*, 389-404.

Hinda, L., Puzenat, E., Houas, A., Ksibi, M., Elaloui, E.,, Guillard C., & Herrmann, J-M. (2002) Photocatalytic degradation of various types of dyes (Alizarin S, Crocein Orange G, Methyl Red, Congo Red, Methylene Blue) in water by UV-irradiated titania. *Applied Catalysis B: Environmental, 39*(1), 75-90.

Hoffmann, M. R., Martin, S. T., Choi, W., & Bahnemann, D. W. (1995). Environmental applications of semiconductor photocatalysis. *Chemical reviews*, *95*(1), 69-96.

Hojamberdiev, M., Czech, B., Göktaş, A. C., Yubuta, K., & Kadirova, Z. C. (2020). SnO_2@ ZnS photocatalyst with enhanced photocatalytic activity for the degradation of selected pharmaceuticals and personal care products in model wastewater. *Journal of Alloys and Compounds*, *827*, 154339.

Holkar, C. R., Jadhav, A. J., Pinjari, D. V., Mahamuni, N. M., & Pandit, A. B. (2016). A critical review on textile wastewater treatments: possible approaches. *Journal of Environmental Management*, *182*, 351-366.

Huang, L., Xu, H., Li, Y., Li, H., Cheng, X., Xia, J., ... & Cai, G. (2013). Visible-light-induced WO 3/gC3N4 composites with enhanced photocatalytic activity. *Dalton Transactions*, 42(24), 8606-8616.

Ibanez, J. G., Rincón, M. E., Gutierrez-Granados, S., Chahma, M. H., Jaramillo-Quintero, O. A., & Frontana-Uribe, B. A. (2018). Conducting polymers in the fields of energy, environmental remediation, and chemical–chiral sensors. *Chemical reviews*, 118(9), 4731-4816.

Iguchi, S., Teramura, K., Hosokawa, S., & Tanaka, T. (2015). Effect of the chloride ion as a hole scavenger on the photocatalytic conversion of CO_2 in an aqueous solution over Ni–Al layered double hydroxides. *Physical Chemistry Chemical Physics*,*17*(27), 17995-18003.

Ilinoiu, E. C., Pode, R., Manea, F., Colar, L. A., Jakab, A., Orha, C., ...& Sfarloaga, P. (2013). Photocatalytic activity of a nitrogen doped TiO_2 modified zeolite in the degradation of Reactive Yellow 125 azo dye. *Journal of the Taiwan Institute of Chemical Engineers*, *44*(2), 270-278.

Irie, H., Miura, S., Kamiya, K., & Hashimoto, K. (2008). Efficient visible light-sensitive photocatalysts: grafting Cu (II) ions onto TiO2 and WO3 photocatalysts. *Chemical Physics Letters*, 457(1-3), 202-205.

Jhaveri, J. H., & Murthy, Z. V. P. (2016). A comprehensive review on anti-fouling nanocomposite membranes for pressure driven membrane separation processes. *Desalination*, 379, 137-154.

Joshni, T. C., & Subramaniam, K. (2011). Enzymatic degradation of azo dyes-a review. *International Journal of Environmental Sciences*,*1*(6), 1250-1260.

Kakarndee, S., & Nanan, S. (2018). SDS capped and PVA capped ZnO nanostructures with high photocatalytic performance toward photodegradation of reactive red (RR141) azo dye. *Journal of Environmental Chemical Engineering*, 6(1), 74-94.

Kakuta, S., Numata, T., & Okayama, T. (2014). Shape effects of goethite particles on their photocatalytic activity in the decomposition of acetaldehyde. *Catalysis Science & Technology*, *4*(1), 164-169.

Katheresan, V., Kansedo, J., & Lau, S. Y. (2018). Efficiency of various recent wastewater dye removal methods: a review. *Journal of Environmental Chemical Engineering*, *6*(4), 4676-4697.

Keen, O. S., Baik, S., Linden, K. G., Aga, D. S., & Love, N. G. (2012). Enhanced biodegradation of carbamazepine after UV/H2O2 advanced oxidation. *Environmental Science &Technology*, 46(11), 6222-6227.

Khalaf, M. N. (2015). Green polymers and environmental pollution control. Apple Academic Press. 436 pp, https://doi.org/10.1201/b19772

Khan, Y., Ahmad, A., Ahmad, N., Mir, F. R., & Schories, G. (2020). Biogenic synthesis of a green tea stabilized PPy/SWCNT/CdS nanocomposite and its substantial applications, photocatalytic degradation and rheological behavior. *Nanoscale Advances*, *2*(4), 1634-1645.

Kiriakidou, F., Kondarides, D. I., & Verykios, X. E. (1999). The effect of operational parameters and TiO2-doping on the photocatalytic degradation of azo-dyes. *Catalysis Today*, *54*(1), 119-130.

Koutavarapu, R., Reddy, C. V., Syed, K., Reddy, K. R., Shetti, N. P., Aminabhavi, T. M., & Shim, J. (2021). Ultra-small zinc oxide nanosheets anchored onto sodium bismuth sulfide nanoribbons as solar-driven photocatalysts for removal of toxic pollutants and photoelectrocatalytic water oxidation. *Chemosphere*, 267, 128559.

Koutavarapu, R., Tamtam, M. R., Myla, C. R., Cho, M., & Shim, J. (2021). Enhanced solar-light-driven photocatalytic properties of novel Z-scheme binary BiPO4 nanorods anchored onto NiFe2O4 nanoplates: Efficient removal of toxic organic pollutants. *Journal of Environmental Sciences*, 102, 326-340.

Koutavarapu, R., Tamtam, M. R., Rao, M. C., Peera, S. G., & Shim, J. (2021). Recent progress in transition metal oxide/sulfide quantum dots-based nanocomposites for the removal of toxic organic pollutants. *Chemosphere*, 129849.

Kshirsagar, A. S., & Khanna, P. K. (2019). $CuSbSe_2/TiO_2$: novel type-II heterojunction nano-photocatalyst. *Materials Chemistry Frontiers*, *3*(3), 437-449.

Kumar, A., & Pandey, G. (2017). Photocatalytic Activity of Co: TiO_2 Nanocomposites and their Application in Photodegradation of Acetic Acid. *Chemical Science*, *6*(3), 385-392.

Kumar, A., Hitkari, G., Singh, S., Gautam, M., & Pandey, G. (2015). Synthesis of Ni-TiO_2 nanocomposites and photocatalytic degradation of oxalic acid in wastewater. *International Journal of Innovative Research in Science, Engineering and Technology*, *4*(12), 12722-12731.

Kumar, R., Travas-Sejdic, J., & Padhye, L. P. (2020). Conducting Polymers-Based Photocatalysis for Treatment of Organic Contaminants in Water. *Chemical Engineering Journal Advances*, 100047.

Kumari, P., Alam, M., & Siddiqi, W. A. (2019). Usage of nanoparticles as adsorbents for wastewater treatment: An emerging trend. *Sustainable Materials and Technologies*, e00128.

Kumari, P., Bahadur, N., & Dumée, L. F. (2020). Photo-catalytic membrane reactors for the remediation of persistent organic pollutants–A review. *Separation and Purification Technology*, 230, 115878.

Li, Q., Xia, Y., Wei, K., Ding, X., Dong, S., Jiao, X., & Chen, D. (2019). Ferroelectric enhanced Z-scheme P-doped gC_3N_4/PANI/$BaTiO_3$ ternary heterojunction with boosted visible-light photocatalytic water splitting. *New Journal of Chemistry, 43*(17), 6753-6764.

Li, S., Zhang, J., Kibria, M. G., Mi, Z., Chaker, M., Ma, D., ...& Rosei, F. (2013). Remarkably enhanced photocatalytic activity of laser ablated Au nanoparticle decorated $BiFeO_3$ nanowires under visible-light. *Chemical Communications*,*49*(52), 5856-5858.

Liang, Y., Wang, X., An, W., Li, Y., Hu, J., & Cui, W. (2019). A g-C_3N_4@ ppy-rGO 3D structure hydrogel for efficient photocatalysis. *Applied Surface Science*, 466, 666-672.

Liao, C. H., Kang, S. F., & Wu, F. A. (2001). Hydroxyl radical scavenging role of chloride and bicarbonate ions in the H_2O_2/UV process. *Chemosphere*, *44*(5), 1193-1200.

Ling, C. M., Mohamed, A. R., & Bhatia, S. (2004). Performance of photocatalytic reactors using immobilized TiO2 film for the degradation of phenol and methylene blue dye present in water stream. *Chemosphere*, 57(7), 547-554.

Liu, H., Du, C., Li, M., Zhang, S., Bai, H., Yang, L., & Zhang, S. (2018). One-pot hydrothermal synthesis of SnO_2/BiOBr heterojunction photocatalysts for the efficient degradation of organic pollutants under visible light. *ACS Applied Materials &Interfaces*, *10*(34), 28686-28694.

Mamba, G., Mamo, M. A., Mbianda, X. Y., & Mishra, A. K. (2014). Nd, N, S-TiO2 decorated on reduced graphene oxide for a visible light active photocatalyst for dye degradation: Comparison to its MWCNT/Nd, N, S-TiO2 analogue. *Industrial & Engineering Chemistry Research*, 53(37), 14329-14338.

Mandal, S., Adhikari, S., Pu, S., Wang, X., Kim, D. H., & Patel, R. K. (2019). Interactive Fe_2O_3/porous SiO_2 nanospheres for photocatalytic degradation of organic pollutants: Kinetic and mechanistic approach. *Chemosphere*, *234*, 596-607.

Mao, K., Wu, X., Min, X., Huang, Z., Liu, Y. G., & Fang, M. (2019). New Efficient Visible-Light-Driven Photocatalyst of Chitin-Modified Titanium Dioxide/Carbon Fiber Composites for Wastewater. *Scientific reports*, *9*(1), 1-9.

Mehraj, O., Mir, N. A., Pirzada, B. M., Sabir, S., & Muneer, M. (2014). In-situ anion exchange synthesis of $AgBr/Ag_2CO_3$ hybrids with enhanced visible light photocatalytic activity and improved stability. *Journal of Molecular Catalysis A: Chemical, 395*, 16-24.

Mishra, A., Mehta, A., Sharma, M., & Basu, S. (2017). Enhanced heterogeneous photodegradation of VOC and dye using microwave synthesized TiO2/Clay nanocomposites: a comparison study of different type of clays. *Journal of alloys and compounds*, 694, 574-580.

Mishra, A., Mehta, A., & Basu, S. (2018). Clay supported TiO_2 nanoparticles for photocatalytic degradation of environmental pollutants: A review. *Journal of Environmental Chemical Engineering*, *6*(5), 6088-6107.

Mishra, A., Mehta, A., Kainth, S., & Basu, S. (2018). Effect of g-C3N4 loading on TiO2/Bentonite nanocomposites for efficient heterogeneous photocatalytic degradation of industrial dye under visible light. *Journal of Alloys and Compounds*, 764, 406-415.

Mitra, M., Ahamed, S. T., Ghosh, A., Mondal, A., Kargupta, K., Ganguly, S., & Banerjee, D. (2019). Polyaniline/reduced graphene oxide composite-enhanced visible-light-driven photocatalytic activity for the degradation of organic dyes. *ACS omega*,*4*(1), 1623-1635.

Moghaddas, S. M. T. H., Elahi, B., & Javanbakht, V. (2020). Biosynthesis of pure zinc oxide nanoparticles using Quince seed mucilage for photocatalytic dye degradation. *Journal of Alloys and Compounds*, *821*, 153519.

Mogyorósi, K., Balázs, N., Srankó, D. F., Tombácz, E., Dékány, I., Oszkó, A., ... & Dombi, A. (2010). The effect of particle shape on the activity of nanocrystalline TiO2 photocatalysts in phenol

decomposition. Part 3: The importance of surface quality. *Applied Catalysis B: Environmental*, *96*(3-4), 577-585.

Moniz, S. J., Shevlin, S. A., Martin, D. J., Guo, Z. X., & Tang, J. (2015). Visible-light driven heterojunction photocatalysts for water splitting–a critical review. *Energy & Environmental Science*, 8(3), 731-759.

Moosvi, S. K., Majid, K., & Ara, T. (2017). Study of thermal, electrical, and photocatalytic activity of iron complex doped polypyrrole and polythiophene nanocomposites. *Industrial & Engineering Chemistry Research*, 56(15), 4245-4257.

Mukhopadhyay, R., Bhaduri, D., Sarkar, B., Rusmin, R., Hou, D., Khanam, R., ... & Ok, Y. S. (2020). Clay–polymer nanocomposites: Progress and challenges for use in sustainable water treatment. *Journal of Hazardous Materials*, *383*, 121125.

Naing, H. H., Wang, K., Li, Y., Mishra, A. K., & Zhang, G. (2020). Sepiolite supported BiVO4 nanocomposites for efficient photocatalytic degradation of organic pollutants: Insight into the interface effect towards separation of photogenerated charges. *Science of The Total Environment*, 722, 137825.

Nasir, M. S., Yang, G., Ayub, I., Wang, S., Wang, L., Wang, X., ... & Ramakarishna, S. (2019). Recent development in graphitic carbon nitride based photocatalysis for hydrogen generation. *Applied Catalysis B: Environmental*, 257, 117855.

Natarajan, S., Bajaj, H. C., & Tayade, R. J. (2018). Recent advances based on the synergetic effect of adsorption for removal of dyes from wastewater using photocatalytic process. *Journal of Environmental Sciences*, *65*, 201-222.

Neghi, N.; Kumar, M.; Burkhalov, D. Synthesis and application of stable, reusable TiO2 polymeric composites for photocatalytic removal of metronidazole: Removal kinetics and density functional analysis. *Chem. Eng. J.* 2019, 359, 963–975/

Ngah, W. W., Teong, L. C., & Hanafiah, M. M. (2011). Adsorption of dyes and heavy metal ions by chitosan composites: A review. *Carbohydrate polymers*, 83(4), 1446-1456.

Ollis, D. F., Pelizzetti, E., & Serpone, N. (1991). Photocatalyzed destruction of water contaminants. *Environmental Science & Technology*, *25*(9), 1522-1529.

Omrani, N., & Nezamzadeh-Ejhieh, A. (2020). A comprehensive study on the enhanced photocatalytic activity of Cu2O/BiVO4/WO3 nanoparticles. *Journal of Photochemistry and Photobiology A: Chemistry*, *389*, 112223.

Papoulis, D., Komarneni, S., Panagiotaras, D., Stathatos, E., Toli, D., Christoforidis, K. C., ... & Katsuki, H. (2013). Halloysite–TiO2 nanocomposites: synthesis, characterization and photocatalytic activity. *Applied Catalysis B: Environmental*, 132, 416-422.

Pardeshi, S. K., & Patil, A. B. (2008). A simple route for photocatalytic degradation of phenol in aqueous zinc oxide suspension using solar energy. *Solar Energy*, *82*(8), 700-705.

Pirzada, B. M., Mehraj, O., Bhat, S. A., & Sabir, S. (2018). Efficient visible-light-driven Photocatalytic activity and enhanced charge transfer properties over Mo-doped WO3/TiO2 nanocomposites. *Journal of Environmental Chemical Engineering*, *6*(2), 3204-3212.

Pirzada, B. M., Mir, N. A., Qutub, N., Mehraj, O., Sabir, S., & Muneer, M. (2015). Synthesis, characterization and optimization of photocatalytic activity of TiO2/ZrO2 nanocomposite heterostructures. *Materials Science and Engineering: B*, *193*, 137-145.

Rajasulochana, P., & Preethy, V. (2016). Comparison on efficiency of various techniques in treatment of waste and sewage water: A comprehensive review. *Resource-Efficient Technologies*, *2*(4), 175-184.

Rameshbabu, R., Kumar, N., Karthigeyan, A., & Neppolian, B. (2016). Visible light photocatalytic activities of ZnFe2O4/ZnO nanoparticles for the degradation of organic pollutants. *Materials Chemistry and Physics*, *181*, 106-115.

Rashid, J., Abbas, A., Chang, L. C., Iqbal, A., Haq, I. U., Rehman, A., ... & Barakat, M. A. (2019). Butterfly cluster like lamellar BiOBr/TiO2 nanocomposite for enhanced sunlight photocatalytic mineralization of aqueous ciprofloxacin. *Science of the Total Environment*, *665*, 668-677.

Rauf, M. A., & Ashraf, S. S. (2009). Fundamental principles and application of heterogeneous photocatalytic degradation of dyes in solution. *Chemical Engineering Journal*, *151*(1-3), 10-18.

Reddy, C. V., Koutavarapu, R., Reddy, I. N., & Shim, J. (2021). Effect of a novel one-dimensional zinc tungsten oxide nanorods anchored two-dimensional graphitic carbon nitride nanosheets for improved solar-light-driven photocatalytic removal of toxic pollutants and photoelectrochemical water splitting. *Journal of Materials Science: Materials in Electronics*, 32(1), 33-46.

Reza, K. M., Kurny, A. S. W., & Gulshan, F. (2017). Parameters affecting the photocatalytic degradation of dyes using TiO 2: a review. *Applied Water Science*, *7*(4), 1569-1578.

Saquib, M., & Muneer, M. (2002). Semiconductor mediated photocatalysed degradation of an anthraquinone dye, Remazol Brilliant Blue R under sunlight and artificial light source. *Dyes and Pigments*, *53*(3), 237-249.

Saquib, M., & Muneer, M. (2003). TiO2-mediated photocatalytic degradation of a triphenylmethane dye (gentian violet), in aqueous suspensions. *Dyes and pigments*, *56*(1), 37-49.

Shafi, A., Ahmad, N., Sultana, S., Sabir, S., & Khan, M. Z. (2019). Ag2S-Sensitized NiO–ZnO Heterostructures with Enhanced Visible Light Photocatalytic Activity and Acetone Sensing Property. *ACS Omega*, *4*(7), 12905-12918.

Silvestri, S., Ferreira, C. D., Oliveira, V., Varejão, J. M., Labrincha, J. A., & Tobaldi, D. M. (2019). Synthesis of PPy-ZnO composite used as photocatalyst for the degradation of diclofenac under simulated solar irradiation. *Journal of Photochemistry and Photobiology A: Chemistry*, 375, 261-269.

Singh, J., & Soni, R. K. (2020). Controlled synthesis of CuO decorated defect enriched ZnO nanoflakes for improved sunlight-induced photocatalytic degradation of organic pollutants. *Applied Surface Science*, 146420.

Soares, E. T., Lansarin, M. A., & Moro, C. C. (2007). A study of process variables for the photocatalytic degradation of rhodamine B. *Brazilian Journal of Chemical Engineering*, *24*(1), 29-36.

Sobana, N., Selvam, K., & Swaminathan, M. (2008). Optimization of photocatalytic degradation conditions of Direct Red 23 using nano-Ag doped TiO2. *Separation and Purification Technology*, 62(3), 648-653.

Song, N., & Jiang, H. L. (2020). Coordinated photodegradation and biodegradation of organic matter from macrophyte litter in shallow lake water: Dual role of solar irradiation. *Water Research,* 172, 115516.

Spanhel, L., & Anderson, M. A. (1991). Semiconductor clusters in the sol-gel process: quantized aggregation, gelation, and crystal growth in concentrated zinc oxide colloids. *Journal of the American Chemical Society*, *113*(8), 2826-2833.

Steplin P., Selvin, S., Ganesh Kumar, A., Sarala, L., Rajaram, R., Sathiyan, A., Princy Merlin, J., & Sharmila, L. I. (2018). Photocatalytic degradation of rhodamine B using zinc oxide activated charcoal polyaniline nanocomposite and its survival assessment using aquatic animal model. *ACS Sustainable Chemistry & Engineering*, 6(1), 258-267.

Stylidi, M., Kondarides, D. I., & Verykios, X. E. (2004). Visible light-induced photocatalytic degradation of Acid Orange 7 in aqueous TiO2 suspensions. *Applied Catalysis B: Environmental*, *47*(3), 189-201.

Sultana, S., Ahmad, N., Ahmad, E., Sabir, S., & Khan, M. Z. (2020). Electrochemical synthesis of novel aluminium oxyhydroxide-decorated MnO 2/chitosan nanocomposite with efficient photocatalytic and antibacterial activity. *Nanotechnology for Environmental Engineering,* 5(2), 1-12.

Szczepanik, B. (2017). Photocatalytic degradation of organic contaminants over clay-TiO2 nanocomposites: A review. *Applied Clay Science*, *141*, 227-239.

Tian, G., Chen, Y., Zhou, W., Pan, K., Tian, C., Huang, X. R., & Fu, H. (2011). 3D hierarchical flower-like TiO 2 nanostructure: morphology control and its photocatalytic property. *Cryst. Eng. Comm*, 13(8), 2994-3000.

Tian, G., Pan, K., Fu, H., Jing, L., & Zhou, W. (2009). Enhanced photocatalytic activity of S-doped TiO2–ZrO2 nanoparticles under visible-light irradiation. *Journal of Hazardous Materials*, *166*(2-3), 939-944.

Vattikuti, S. P., Reddy, P. A. K., Shim, J., &Byon, C. (2018). Visible-light-driven photocatalytic activity of SnO2–ZnO quantum dots anchored on g-C3N4 nanosheets for photocatalytic pollutant degradation and H2 production. *ACS Omega*, *3*(7), 7587-7602.

Wahid, F., Duan, Y. X., Hu, X. H., Chu, L. Q., Jia, S. R., Cui, J. D., & Zhong, C. (2019). A facile construction of bacterial cellulose/ZnO nanocomposite films and their photocatalytic and antibacterial properties. *International Journal of Biological Macromolecules*, *132*, 692-700.

Wang, J., & Wang, S. (2016). Removal of pharmaceuticals and personal care products (PPCPs) from wastewater: a review. *Journal of Environmental Management*, 182, 620-640.

Wang, L., & Wang, A. (2007). Adsorption characteristics of Congo Red onto the chitosan/montmorillonite nanocomposite. *Journal of Hazardous Materials*, 147(3), 979-985.

Wang, X. J., Yang, W. Y., Li, F. T., Zhao, J., Liu, R. H., Liu, S. J., & Li, B. (2015). Construction of amorphous TiO2/BiOBr heterojunctions via facets coupling for enhanced photocatalytic activity. *Journal of Hazardous Materials*, *292*, 126-136.

Wang, X., Jia, J., & Wang, Y. (2011). Degradation of CI Reactive Red 2 through photocatalysis coupled with water jet cavitation. *Journal of Hazardous Materials*, *185*(1), 315-321.

Weldegebrieal, G. K. (2020). Synthesis method, antibacterial and photocatalytic activity of ZnO nanoparticles for azo dyes in wastewater treatment: A review. *Inorganic Chemistry Communications*, 120, 108140.

Weon, S., He, F., & Choi, W. (2019). Status and challenges in photocatalytic nanotechnology for cleaning air polluted with volatile organic compounds: visible light utilization and catalyst deactivation. *Environmental Science: Nano*, *6*(11), 3185-3214.

Worch, E. (2012). Adsorption technology in water treatment: fundamentals, processes, and modeling. Walter de Gruyter.https://doi.org/10.1515/9783110240238

Xie, M., & Zhang, T. (2020). A novel efficient visible-light-driven double Z-scheme PANI/Ag 3 PO 4/CNO heterojunction photocatalyst mediated by PANI and in situ grown AgNPs. *Journal of Materials Science*, *55*(9), 3974-3990.

Yang, X., Cai, H., Bao, M., Yu, J., Lu, J., & Li, Y. (2018). Insight into the highly efficient degradation of PAHs in water over graphene oxide/Ag3PO4 composites under visible light irradiation. *Chemical Engineering Journal*, *334*, 355-376.

Yang, Y., Ma, S., Qu, J., Li, J., Liu, Y., Wang, Q., ... & Wu, J. (2021). Transforming type-II Fe2O3@ polypyrrole to Z-scheme Fe2O3@ polypyrrole/Prussian blue via Prussian blue as bridge: Enhanced activity in photo-Fenton reaction and mechanism insight. *Journal of Hazardous Materials*, 405, 124668.

Yao, Y., Cai, Y., Lu, F., Qin, J., Wei, F., Xu, C., & Wang, S. (2014). Magnetic ZnFe2O4–C3N4 hybrid for photocatalytic degradation of aqueous organic pollutants by visible light. *Industrial & Engineering Chemistry Research*, *53*(44), 17294-17302.

Ye, J., Liu, S. Q., Liu, W. X., Meng, Z. D., Luo, L., Chen, F., & Zhou, J. (2019). Photocatalytic Simultaneous Removal of Nitrite and Ammonia via a Zinc Ferrite/Activated Carbon Hybrid Catalyst under UV–Visible Irradiation. *ACS Omega*, *4*(4), 6411-6420.

Younes, I., & Rinaudo, M. (2015). Chitin and chitosan preparation from marine sources. Structure, properties and applications. *Marine drugs*, *13*(3), 1133-1174.

Yu, J. C., Yu, J., Ho, W., Jiang, Z., & Zhang, L. (2002). Effects of F-doping on the photocatalytic activity and microstructures of nanocrystalline TiO2 powders. *Chemistry of materials*, *14*(9), 3808-3816.

Zhai, L., & McCullough, R. D. (2004). Regioregular polythiophene/gold nanoparticle hybrid materials. *Journal of Materials Chemistry*, 14(2), 141-143.

Zhang, J., Li, L., Xiao, Z., Liu, D., Wang, S., Zhang, J., ... & Zhang, W. (2016). Hollow sphere TiO2–ZrO2 prepared by self-assembly with polystyrene colloidal template for both photocatalytic degradation and H2 evolution from water splitting. *ACS Sustainable Chemistry & Engineering*, *4*(4), 2037-2046.

Zhang, Y., Crittenden, J. C., Hand, D. W., & Perram, D. L. (1996). Destruction of organic compounds in water using supported photocatalysts. *Journal of Solar Energy Engineering*, 123-129.

Zhang, Y., Gan, H., & Zhang, G. (2011). A novel mixed-phase TiO2/kaolinite composites and their photocatalytic activity for degradation of organic contaminants. *Chemical Engineering Journal*, 172(2-3), 936-943.

Zhao, H., Li, G., Tian, F., Jia, Q., Liu, Y., & Chen, R. (2019). g-C3N4 surface-decorated Bi2O2CO3 for improved photocatalytic performance: Theoretical calculation and photodegradation of antibiotics in actual water matrix. *Chemical Engineering Journal*, *366*, 468-479.

Zhao, W., Wang, Y., Wang, A., Qian, J., Zhu, W., Dou, S., ... & Chen, A. (2017). Novel Bi 2 O 2 CO 3/polypyrrole/gC 3 N 4 nanocomposites with efficient photocatalytic and nonlinear optical properties. *RSC Advances*, 7(13), 7658-7670.

Zhu, J., Deng, Z., Chen, F., Zhang, J., Chen, H., Anpo, M., ... & Zhang, L. (2006). Hydrothermal doping method for preparation of Cr3+-TiO2 photocatalysts with concentration gradient distribution of Cr3+. *Applied Catalysis B: Environmental*, *62*(3-4), 329-335.

Zhu, Y., Wan, T., Wen, X., Chu, D., & Jiang, Y. (2019). Tunable Type I and II heterojunction of CoOx nanoparticles confined in g-C3N4 nanotubes for photocatalytic hydrogen production. Applied Catalysis B: Environmental, 244, 814-822.

Zhu, Y., Xu, S., & Yi, D. (2010). Photocatalytic degradation of methyl orange using polythiophene/titanium dioxide composites. *Reactive and Functional Polymers*, *70*(5), 282-287.

Zia, J., Aazam, E. S., & Riaz, U. (2020). Highly efficient visible light driven photocatalytic activity of MnO2 and Polythiophene/MnO2 nanohybrids against mixed organic pollutants. *Journal of Molecular Structure*, *1207*, 127790.

Supplementary Information

Visible light-conducting polymer nanocomposites as efficient photocatalysts for the treatment of organic pollutants in wastewater

Nafees Ahmad [1,2], Jerry Anae[1], Mohammad Zain Khan[2], Suhail Sabir[2], Xiao Jin Yang[3,4], Vijay Kumar Thakur[5], Pablo Campo[1], Frederic Coulon[1*]

[1] School of Water, Energy and Environment, Cranfield University, Cranfield, MK 43 0AL, UK

[2]Environmental Research Laboratory, Department of Chemistry, Aligarh Muslim University, Aligarh, India, 202002

[3]State Key Laboratory of Chemical Resource Engineering, Beijing Advanced Innovation Center for Soft Matter Science and Engineering, Beijing University of Chemical Technology, Beijing 100029, China

[4]State Key Laboratory of Organic-Inorganic Composites, Beijing University of Chemical Technology, Beijing, 100029, PR China

[5]Biorefining and Advanced Materials Research Centre, Scotland's Rural College, Edinburgh, EH9 3JG, UK

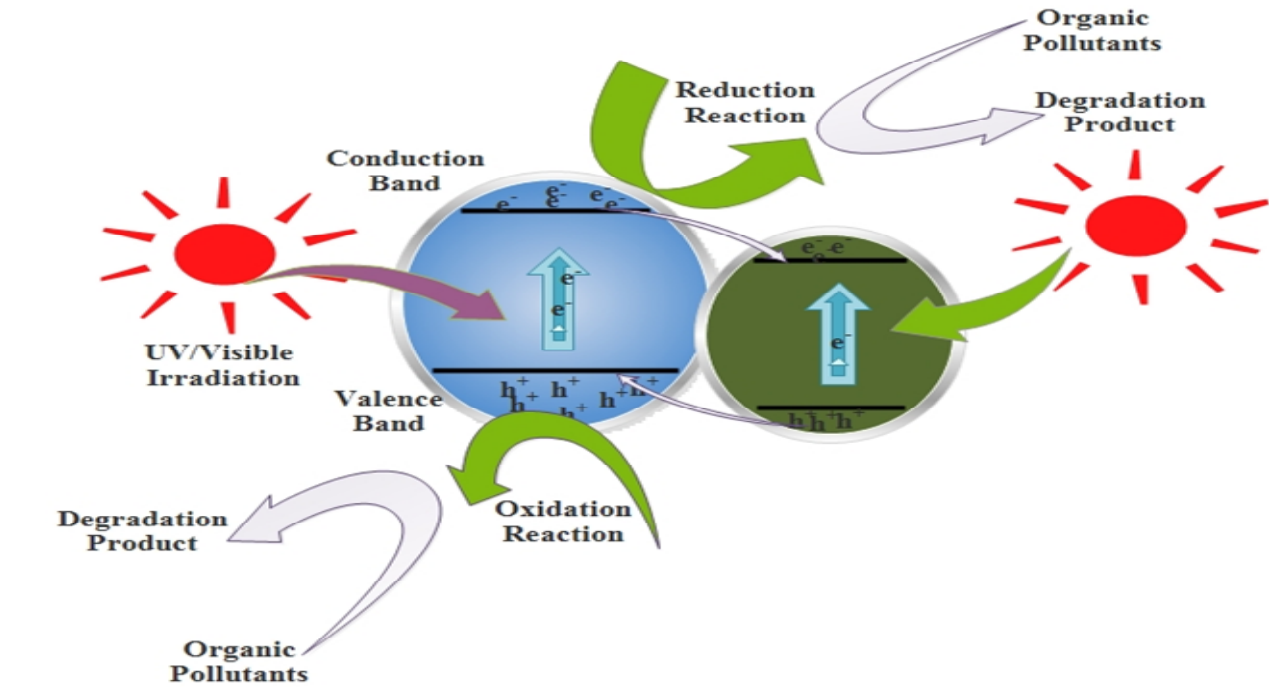

Fig. S1: General mechanism of the photocatalysis process in case of coupled heterojunction

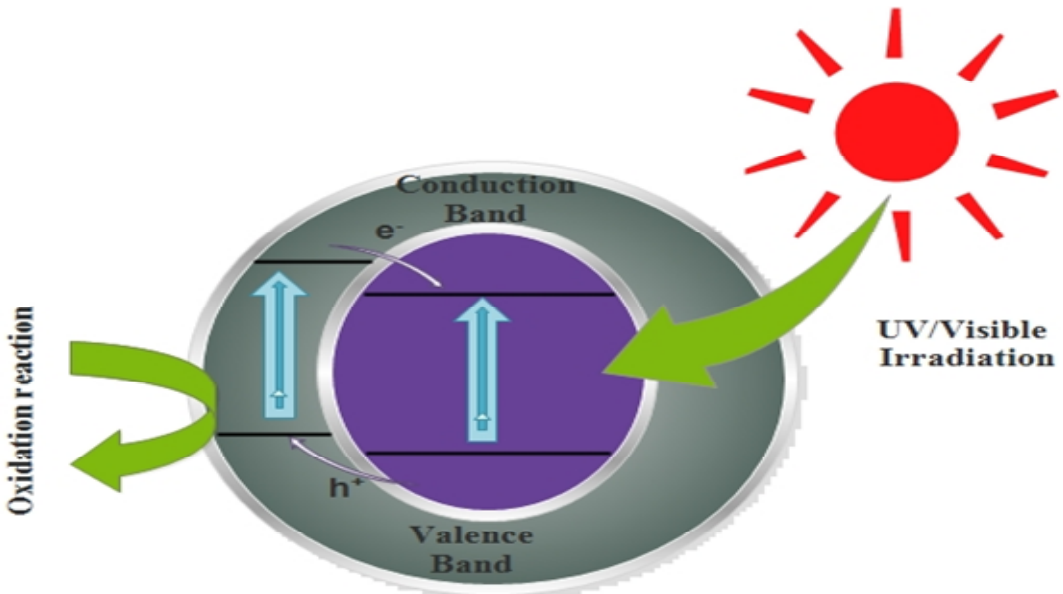

Fig. S2: General mechanism of the photocatalysis process in case of capped heterojunction

Table S1: Various conducting polymer-semiconductor nanocomposites for used for the photodegradation.

S.No	Photocatalyst	Bandgap energy	Light Intensity	Targeted pollutants	Effic.	Exposure Time (Min)	Reference
1	Polypyrrole/Zinc ferrite-g-C_3N_4	Polypyrrole-2.1eV Zinc ferrite-1.9eV g-C_3N_4- 2.7 eV	Xenon Lamp (150 W)	Ciprofloxin	92%	120	Das et al. 2020
2	Polypyrrole Nanostructure	2.41eV	Xenon Lamp (300 W)	Phenol Methyl Orange	100% 80%	270 300	Yuan et al. 2019
3	TiO_2/CDs/PANI	1.5-3.2eV	LED (50 W)	Rhodamine B	99%	90	Feizpoor et al. 2018
4	PANI/BiOBr/$ZnFe_2O_4$	PANI-1.97eV BiOBr-2.78eV $ZnFe_2O_4$-1.89eV	High pressure (Hg Lamp)	Rhodamine B Nitrobenzene	99% 87%	30	Zhang et al. 2020
5	BiOBr-GO-polyaniline	BiOBr-2.72eV GO-2.50eV Polyaniline-2.70eV	Halogen Lamp (150 W)	Phenol	89%	60	Lui et al. 2019
6	Polyaniline/CdS -Hydrolyzed Pectin	CdS-2.4eV	UV Lamp (8 W)	Rhodamine B	86%	150	Alipour et al. 2019
7	Polyaniline-MIL-100(Fe)	Polyaniline-2.70eV MIL-100(Fe) 2.77 eV Composites- 2.47-2.29eV	Xe Lamp (300 W)	Cr(IV) Tetracycline	100% 84%	90 120	Chen et al. 2020
8	g-C_3N_4-Polyaniline co-modified TiO_2	g-C_3N_4- 2.7 eV Polyaniline-2.1eV TiO2-3.2eV	Xe Lamp (120 W)	Tetrabromobis-phenol A	92%	120	Zhou et al. 2020
9	Porphyrin/ $ZnFe_2O_4$/ Polythiophene	$ZnFe_2O_4$-2.18 eV ZnFe/PTh-1.95eV ZnFe/PTh/Porphyrin-1.85eV	LED (5W)	Methylene Blue Methyl Orange	94%	180	Kharazi et al. 2018
10	Polythiophene/ TiO_2	Polythiophene-2.6ev TiO_2- 3.2eV	Linear Halogen Lamp (360 W)	Methyl Orange	80.3 %	600	Zhu et al. 2010

Table S2: Example of various conducting polymer-biopolymer based composite for photocatalytic degradation of organic pollutants

	Photocatalyst	Bandgap energy	Target Pollutants	Efficiency	Irradiation Time (Min)	Light Intensity	Reference
1	Polypyrrole Grafted Chitosan-decorated CDs	Polypyrrole 2.4ev	2-Chloro phenol	96.7%	90	Sunlight	Midya et al. 2019
2	Polypyrrole/SnO_2-Chitin	Polypyrrole-2.1ev SnO2 3.4ev	Rh B	86.8%	220	Halogen Lamp (500 W)	Bano et al. 2019
3.	Polyaniline-Chitosan-Ag	--------	Ponceau BS	81%	80	Halogen Lamp (500 W)	Sultana et al. 2017
4	Polypyrrole/Chitosan-ZnO	Composites-2.4 eV	Reactive Orange-16	83%	80	Halogen Lamp (500 W)	Ahmad et al. 2019
5	Polyaniline/Cellulose-Ni	Composites. 2.2eV	Reactive Orange -16	91%	60	Halogen Lamp (500 W)	Ahmad et al. 2018